April 2018

Targeting the Hsp90/Aha1 Complex for the Treatment of Tauopathies

Lindsey Brooke Shelton
University of South Florida, lshelton@health.usf.edu

Targeting the Hsp90/Aha1 Complex for the Treatment of Tauopathies

by

Lindsey Brooke Shelton

A dissertation submitted in partial fulfillment
of the requirements for the degree of
Doctor of Philosophy
with a concentration in Neuroscience
Department of Molecular Medicine
Morsani College of Medicine
University of South Florida

Major Professor: Thomas Taylor-Clark, Ph.D.
Co-Major Professor: Laura Blair, Ph.D.
Danielle Gulick, Ph.D.
Daniel Lee, Ph.D.
Lynn Wecker, Ph.D.

Date of Approval:
April 11, 2018

Keywords: Aha1, Alzheimer's disease, chaperones, Hsp90, tauopathies

DEDICATION

I would like to dedicate this work to my late mentor, Dr. Chad Dickey who sadly lost his battle with cancer in November of 2016. Without the guidance, support, and tough-love from Dr. Dickey I would not be the scientist I am today. I would also like to dedicate this work to my mother Carla Knight, my father Randy Shelton, and my husband Christian Kirkland. Without your love and support I would not be where I am at today. Thank you.

ACKNOWLEDGMENTS

I would like to acknowledge several people for the roles they played throughout my graduate career. Specifically, Jeremy Baker for helping me through all the tough times and being a friend as we navigated grad school together. Dr. Thomas Taylor-Clark who stepped in to be my mentor after the passing of Dr. Dickey and continues to provide me with constant support and motivation. Dr. Laura Blair who kept the Dickey lab running smoothly through the rocky times. Lastly, I would like to thank Drs. Gulick, Lee, and Wecker for being on my committee and providing me with valuable feedback and encouragement.

TABLE OF CONTENTS

LIST OF TABLES

LIST OF FIGURES

ABSTRACT

The microtubule associated protein, tau, is involved in regulating microtubule stability and axonal transport. When tau becomes hyperphosphorylated it can disassociate from the microtubules and start to aggregate. These tau aggregates are the hallmarks of many diseases known as tauopathies. The heat shock protein 90 kDa (Hsp90) chaperone network is highly involved in modulating client proteins, including tau. However, during aging and disease the Hsp90 chaperone network becomes highly imbalanced with some Hsp90/co-chaperone complexes increasing, while others are repressed. This imbalance in Hsp90/co-chaperone complexes could result in a worsening of tau pathology in Alzheimer's disease.

Hsp90 inhibition has been of interest as a potential therapeutic for tauopathies for many years. However, issues with toxicity and bioavailability have dampened enthusiasm for Hsp90 as a viable therapeutic target. Hsp90 co-chaperones are currently being investigated for as potential therapeutic targets for tauopathies, with the hope that targeting co-chaperones will lead to more specific targeting without toxicity. One co-chaperone that has the potential to become a therapeutic target for tauopathies is the activator of Hsp90 ATPase homolog 1 (Aha1).

Aha1 is the only known stimulator of the ATPase of Hsp90, so targeting this particular co-chaperone could potentially mimic the effects of Hsp90 inhibition with more

specificity. In this study we found that Aha1 enhanced Hsp90-mediated tau aggregation and increased insoluble tau accumulation *in vitro*. Additionally, a novel Aha1 inhibitor was able to reduce the formation of insoluble tau *in vitro*. We also investigated the effects of Aha1 overexpression in the rTg4510 mouse model, which is a tauopathy model that stably overexpresses the P301L mutation of tau. Overexpression of Aha1 in these mice increased the accumulation of insoluble and oligomeric tau. Furthermore, Aha1 overexpression led to cognitive deficits and neurotoxicity. Due to the effect of Aha1 overexpression on tau we wanted to investigate the effects of Aha1 knock-down in the rTg4510 mice. Incredibly, Aha1 knock-down led to reductions in pathological Gallyas silver positive tau tangles and was able to rescue neuronal loss. Overall, this work highlights Aha1 as an important regulator of tau pathology through Hsp90. The Hsp90/Aha1 complex could provide a novel therapeutic target for the treatment of tauopathies.

Chapter One[1]:

Imbalances in the Hsp90 chaperone machinery: Implications for tauopathies

1.1 Abstract

The ATP-dependent 90kDa heat shock protein, Hsp90, is a major regulator of protein triage, from assisting in nascent protein folding to refolding or degrading aberrant proteins. Tau, a microtubule associated protein, aberrantly accumulates in Alzheimer's disease (AD) and other neurodegenerative diseases, deemed tauopathies. Hsp90 binds to and regulates tau fate in coordination with a diverse group of co-chaperones. Imbalances in chaperone levels and activity, as found in the aging brain, can contribute to disease onset and progression. For example, the levels of the Hsp90 co-chaperone, FK506-binding protein 51 kDa (FKBP51), progressively increase with age. *In vitro* and *in vivo* tau models demonstrated that FKBP51 synergizes with Hsp90 to increase neurotoxic tau oligomer production. Inversely, protein phosphatase 5 (PP5), which dephosphorylates tau to restore microtubule-binding function, is repressed with aging and activity is further repressed in AD. Similarly, levels of cyclophilin 40 (CyP40) are reduced in the aged brain and further repressed in AD. Interestingly, CyP40 was shown to breakup tau aggregates *in vitro* and prevent tau-induced neurotoxicity *in vivo*. Moreover, the only known stimulator of Hsp90 ATPase activity, Aha1, increases tau aggregation and toxicity. While the levels of Aha1 are not significantly altered with aging, increased levels have been found in AD brains. Overall, these changes in the Hsp90 heterocomplex could drive tau deposition and neurotoxicity. While the relationship of tau and Hsp90 in coordination with these co-

chaperones is still under investigation, it is clear that imbalances in these proteins with aging can contribute to disease onset and progression. This chapter highlights the current understanding of how the Hsp90 family of molecular chaperones regulates tau or other misfolded proteins in neurodegenerative diseases with a particular emphasis on the impact of aging.

---

[1]Portions of this work were previously published (Shelton LB et al., 2018) and are used with permission of the publisher.

1.2 Introduction

Aging is the biggest risk factor for developing a neurodegenerative disease, but the specific factors which cause these predominantly sporadic diseases are still under investigation (1). As cells within the body age, the cellular homeostasis network must deal with an increasing amount of misfolded and aggregated proteins that can pathogenically accumulate leading to cell death. Aging is caused by compromised cellular homeostasis, fitness, and plasticity, leading to degeneration and cell death in vital organs. According to the 'garbage catastrophe' hypothesis, aged differentiated cells lose the capacity to dispose of damaged and malfunctioning proteins (2). Such damaged proteins can assume cytotoxic properties, and their constant removal is thus essential for cell survival. Not only does aging lead to an increased likelihood of protein misfolding and aggregation, it is compounded by a decrease in the efficiency of the protein degradation machinery. The activity of both the proteasome, which is the main mechanism of protein degradation (3, 4), and chaperone-mediated autophagy (CMA; (5)) is significantly impaired with aging and is especially pronounced in post-mitotic cells, such as neurons, potentially resulting

in neurodegenerative disease (2). Fortunately, there is a system in place to help the body maintain proteostasis in times of stress and disease: the molecular chaperone network (6). This network is comprised of a diverse family of proteins which contains members that are constitutively expressed to help in normal cell maintenance as well as members that become activated during times of stress. All of these chaperones assist in various ways to help fold, refold and degrade misfolded proteins.

The molecular chaperone network is comprised of diverse families of heat shock proteins (Hsps) that are divided based on their molecular mass. The small Hsps regulate general protein aggregation, Hsp40s regulate Hsp70 ATP hydrolysis, Hsp70 folds proteins during translation, and Hsp90 maintains and triages a subset of clients (7, 8). While Hsp70 and Hsp90 perform many overlapping roles in the cell, Hsp90 shows more client selectivity. Hsp90 requires ATP to perform these functions including protein degradation, protein folding, prevention of protein aggregation, and protein modification (9). These regulatory processes are particularly important for intrinsically disordered proteins (IDPs), which have a high propensity to aggregate (10).

Hsp90 binds to one of these IDPs, tau, in a broad region that includes aggregation prone areas (11). Tau normally functions to stabilize the microtubules and regulate axonal transport (12). The pathological accumulation of tau is a hallmark in several neurodegenerative disorders collectively termed tauopathies (13); a series of diseases including Alzheimer's disease (AD), progressive supranuclear palsy (PSP), Pick's disease, and chronic traumatic encephalopathy (CTE; (12)). Currently there are no treatment options available that regulate tau pathogenesis (14), therefore more work needs to be done to identify potential tau regulating therapeutic strategies.

A promising avenue to target tau is through Hsp90 inhibition. In fact, Hsp90 ATPase-inhibitors rapidly degrade tau aggregates *in vivo* (15, 16), but these inhibitors have not yet been successful in clinical trials due to lack of efficacy and associated toxicities (17–19). However, Hsp90 regulates tau and other aggregating proteins in coordination with a diverse group of co-chaperones (10). In fact, the levels of many of these co-chaperones have been shown to change with aging, which can alter the fate of tau and potentially contribute to disease onset or severity (20, 21). It is possible that a more successful treatment strategy may be found by a therapeutic aimed toward regulating these co-chaperones or Hsp90/co-chaperone heterocomplexes (22, 23). This chapter discusses the involvement of Hsp90 and its co-chaperones in disease and how alterations in levels and activity with aging can affect this process (Table 1.1). Current Hsp90 therapeutic interventions for neurodegenerative diseases will also be reviewed.

1.3 Hsp90

Hsp90 is critical to maintaining proteostasis (21) and accounts for up to 6% of all protein within the cell during times of stress (24, 25). Hsp90 consists of three domains: an N-terminal ATP-binding domain, a middle domain, and a C-terminal domain responsible for the inherent dimerization of the protein (26). Hsp90 requires ATP in order to dimerize and properly assist in protein folding. The Hsp90 ATPase cycle consists of four stages: the ATP-bound state, an initial intermediate state (I1), a second intermediate state (I2), and finally a closed state in which ATP hydrolysis occurs (26). There are several different isoforms of Hsp90: cytosolic Hsp90, which includes Hsp90α (stress-inducible) and Hsp90β (constitutively active); an endoplasmic reticulum (ER) isoform, gluclose-regulated protein 94 (GRP94); and a mitochondrial associated isoform, tumor necrosis

factor receptor associated protein 1 (TRAP1) (24, 27). Very little is known about the organelle specific Hsp90 isoforms, so this chapter will focus on cytosolic Hsp90.

The two different cytosolic forms of Hsp90 are 86% genetically identical and have 93% amino acid sequence homology, showing lots of similarities in structure and function. However, there are some differences that set these two isoforms apart. The first difference is the viability of Hsp90 knock-out mice. Mice lacking Hsp90β are embryonically lethal and do not survive past day 9, whereas mice lacking Hsp90α are viable but leads to sterility in male mouse (28, 29). There are also some differences in the cellular functions of Hsp90α and Hsp90β. Hsp90α is involved in growth promotion, cell cycle regulation, stress-induced cytoprotection, and cancer cell invasiveness; whereas Hsp90β is involved with early embryonic development, germ cell maturation, cytoskeletal stabilization, cellular transformation, signal transduction, and long-term cell adaptation (30, 31). While there are some general functional differences between the two cytosolic isoforms more studies are needed to better understand the role of these different isoforms on tau pathology.

Alterations in chaperone expression are commonly seen in aging, leading to complications within the Hsp90 chaperone network. In fact, recent work has shown the levels of many Hsp90 co-chaperones are also altered in the aged brain (21). These co-chaperones are necessary for client selection and triage. There are two main categories of Hsp90 co-chaperones: tetratricopeptide repeat (TPR) and non-TPR containing (32). Therefore, changes in Hsp90 levels are part of a larger imbalance in the chaperone network, which contribute to aging and age-related neurodegenerative disorders.

1.4 Aha1

The activator of Hsp90 ATPase homolog 1 (Aha1) works as a co-chaperone to stimulate the ATPase function of Hsp90 to regulate the folding and activation of client proteins. Pearl and Prodromou were the first to identify the role of Aha1 as a stimulatory co-chaperone of Hsp90 (33). Aha1 is a relatively small protein of 38kDa that is highly conserved from yeast to man (33, 34). There is also an Aha1-related protein, Aha2, which can only be found in higher eukaryotes although this protein has not been well characterized (35). Aha1 is highly expressed throughout tissues such as the kidney, brain, heart, and skeletal muscles and is mainly localized to the cyctoplasm within cells (35). Aha1 knock-out mice are available and viable but there is currently no information on any phenotypic deficits (The Jackson Laboratory; Stock No: 029805).

Aha1 interacts with Hsp90 independent of its nucleotide status and allows the Hsp90 ATPase cycle to skip the I1 phase, thus accelerating the progression of the ATPase cycle dramatically (26, 36). Interestingly, only one Aha1 protein is required to fully stimulate the ATPase activity of Hsp90 even though there are two binding pockets on each Hsp90 dimer (36). One study suggests that SUMOlyation of a conserved lysine on Hsp90 (K191) facilitates the recruitment of Aha1 (37). Another study found that c-Abl phosphorylation of the tyrosine residue Y223 in human Aha1 promotes its interaction with Hsp90 (38). Perhaps both of these post-translational modifications need to occur for Hsp90 and Aha1 to interact, however, it is possible that either of these PTMs are sufficient. While the c-Abl tyrosine kinase is important in promoting the interaction between Aha1 and Hsp90, it also plays a significant role in tau phosphorylation. One study has shown that amyloid-β-peptide (Aβ) activates c-Abl, which then goes on to

phosphorylate tau through Cdk5 activation (39). This same study found that inhibition of c-Abl expression via shRNA decreased both AT8 and PHF1 tau in the APPswe/PSEN1ΔE9 transgenic mouse (39). These findings suggest that c-Abl could be a link between tau and Aha1, because when c-Abl levels are increased, there is an increased association between Aha1 and Hsp90 as well as an increase in tau phosphorylation and aggregation, but more studies are needed to elucidate the specifics of these interactions.

Aha1 has been investigated for its role in several diseases such as cancer, cystic fibrosis, and more recently, tauopathies. In cancer cells, when c-Abl is inhibited, Aha1 is unable to interact with Hsp90, which allows the cancer cells to become hypersensitized to other treatments, such as Hsp90 inhibition (38). Cystic fibrosis was the first disease that Aha1 was implicated in and, studies have shown that downregulation of Aha1 is able to rescue the translocation of the mutant form of cystic fibrosis transmembrane conductance regulator (CFTR) ΔF508 (40). This provides additional support for targeting Aha1, as suppression of Aha1 is beneficial in multiple diseases. It is interesting to note that Aha1 levels have been shown to increase with AD. In fact, we have found that Aha1 levels in the medial temporal gyrus of human brain correlated with increased tau Braak staging (41). In the same study, we found that high levels of Aha1 in a tau transgenic mouse model increased tau oligomers as well as neuronal loss concomitant with cognitive deficits (41). Since Aha1 levels are repressed in aging, but are abnormally preserved in AD, tau aggregation could be accelerated in part by Aha1 in the AD brain. Thus, treatments which reduce Aha1 may be beneficial for diseases such as AD and cystic fibrosis.

While the Aha1/Hsp90 complex and the impact on tau is the focus of this thesis, there are many other important co-chaperones that play a role in the complicated dynamics of the Hsp90 chaperone network. The rest of the Hsp90 co-chaperones and their relationship to tau will be discussed below.

1.5 TPR co-chaperones

TPR-containing Hsp90 co-chaperones interact with the C-terminal MEEVD peptide motif on Hsp90 (27). Since Hsp90 functions as a dimer, two TPR-containing co-chaperones could interact simultaneously. However, these interactions are dependent on the isoform of Hsp90 and the repertoire of expressed co-chaperones. In fact, co-chaperones do compete for binding to Hsp90 (42, 43). This competition can have beneficial or detrimental effects on tau pathology. Known examples include co-chaperones which interact with Hsp90 to promote the degradation of aberrant tau or others which drive tau oligomerization and aggregation. Therefore, an imbalance in protein levels with aging and AD compound this already complex competition for binding Hsp90 to regulate tau fate (Fig. 1.1). Here, we will describe these TPR-co-chaperones, and how their interaction with Hsp90 regulates tau.

1.5.1 Immunophilins and Immunophilin homologs

Hsp90 interacts with six immunophilins that display peptidyl-prolyl isomerase (PPIase) activity through TPR domains including cyclophilin 40 (CyP40) and five FK506-binding proteins: FKBP51, FKBP52, FKBP36, FKBP38, FKBPL/WISp39 (44–47). These PPIases regulate the twisting of proline bonds through stabilization of the *cis-trans* transition state and accelerate the isomerization process. This is particularly important for

tau, which has 40 proline residues that regulate phosphorylation and aggregation propensity (48). Hsp90 also interacts with two immunophilin homologs: protein phosphatase 5 (PP5) and XAP2/FKBP37. Altered levels of many of these immunophilins and immunophilin-like proteins have been found in aging and AD (Table 1.1), which could skew the competition dynamics for Hsp90 binding (discussed later in this chapter) and may promote toxic tau accumulation.

1.5.1.1 CyP40

An interesting PPIase, CyP40, decreases in aging and is further repressed in AD (21). CyP40 was recently shown to disaggregate tau fibrils *in vitro* and prevents toxic tau accumulation *in vivo* preserving memory, demonstrating a neuroprotective role for CyP40 in the brain (49). The PPIase activity of CyP40 is slightly repressed when bound to Hsp90, but under cellular stress CyP40 can release from Hsp90 increasing its isomerase and chaperone activity (50). However, as CyP40 levels decrease with aging, it is possible that the pool of free CyP40 is not sufficient to help disentangle aggregating proteins, like tau.

1.5.1.2 FKBP51

Contrary to the neuroprotective effects of CyP40, two FK506-binding proteins (FKBPs) have been shown to stimulate toxic tau aggregation (20, 51, 52). One of these, FKBP51, coordinates with Hsp90 to preserve toxic tau oligomers *in vivo* (Blair et al., 2013). In fact, mice lacking FKBP51 have decreased tau levels in the brain (20, 53). However, throughout aging, FKBP51 levels progressively increase and are further increased in AD brain samples (Table 1.1) (20, 54). Previous studies have also shown that FKBP51 can form complexes with tau in both human AD brain samples and control

samples (53). Additionally, this study showed that FKBP51 was able to stabilize microtubules, suggesting a novel and unique function for FKBP51 (53). Taken together, the increase in FKBP51 in aging and AD suggest that targeting FKBP51 could offer a potential therapeutic strategy for tauopathies such as AD.

1.5.1.3 FKBP52

FKBP52 interacts both physically and functionally with tau and promotes tau aggregation *in vitro* (51, 55). FKBP52 induces oligomers from both P301L and truncated wild-type tau. Interestingly, this oligomerization is not due to the PPIase activity of FKBP52, instead the oligomerization of tau appears to occur via molecular interaction (52). FKBP52 can also induce aggregation of a truncated form of tau that appears to have prion like behavior, suggesting a possible mechanism for the spread of tau pathology throughout the brain in diseases such as AD (51). However, it is interesting to note that FKBP52 levels are lower in the cortex of AD patients' brains (Table 1.1) (21, 55).

1.5.1.4 FKBP36, FKBP38, and FKBPL

There are several other FKBPs that act as co-chaperones to Hsp90 including FKBP36, FKBP38, and FKBPL (WISp39), however their relationship to tau, if any, is still unknown at this point and so they will not be discussed in detail.

1.5.1.5 XAP2

XAP2, otherwise known as FKBP37 or Aryl hydrocarbon receptor interacting protein (AIP), contains a PPIase homologous domain. While a direct role of XAP2 in tau pathogenesis has not been described, studies have shown that XAP2 is activated by

histone deacetylase (HDAC) 6, which has been linked to pathogenic tau (56–58). In addition, XAP2 coordinates with Hsp90 to regulate glucocorticoid receptor signaling (59), which has also been implicated in the production of pathogenic tau (60). Additional studies are needed to determine the direct or indirect effects of XAP2 on tau pathology.

1.5.1.6 PP5

Another member of this family, protein phosphatase 5 (PP5), is repressed in aging. PP5 is contains a PPIase homology domain, but does not display classical PPIase activity, since it can bind FK506 (61). Instead, PP5 acts as a Ser/Thr phosphatase, which activates when bound to Hsp90 (62). PP5 activity has been shown to be repressed in AD (Table 1.1) (63). Studies have shown that PP5 is able to dephosphorylate tau at several phosphorylation sites connected to AD pathology (64). Further studies are needed to better understand if the upregulation of PP5 could be used to slow or prevent tau pathogenesis.

1.5.2 Hop

The Hsp70-Hsp90 organizing protein, otherwise known as Hop and sometimes STIP1 (stress inducible protein 1), is involved in helping transfer client proteins from the early stages of protein maturation involving Hsp70 and Hsp40 to the later stages of the cycle involving Hsp90 (65). As such, Hop plays a crucial role in the maturation of client proteins, like tau. A previous study found that when Hop was depleted using siRNA, there was an accumulation of tau (66). This suggests that Hop is necessary for tau clearance via Hsp70/Hsp90. In fact, loss-of-function mutations in Hop drive toxic tau accumulation

in a fly model of tauopathy (67). Together these studies demonstrate a protective role of Hop in a tauopathic brain.

1.5.3 CHIP

C-terminus of Hsc70-interacting protein (CHIP) is highly involved in the Hsp70-Hsp90 machinery acting not only as a co-chaperone, but also as an E3 ubiquitin ligase responsible for ubiquitin-dependent proteasomal degradation (68). CHIP has many roles within the cell including stress-response activation, protein triage, and restitution of the stress response (69). CHIP has been linked to several neurodegenerative disorders including Huntington's disease, Parkinson's disease and AD as well as other diseases such as cystic fibrosis and cancer (68, 69). In tauopathic mice, CHIP regulates the removal of tau species that have undergone abnormal phosphorylation and folding (69). Additionally, silencing CHIP via siRNA, led to a massive increase in tau levels (70). Similarly, CHIP/*Stub1*-knockout mice have increased accumulation of phospho- and total tau species (Table 1.2) (71). Overexpression of CHIP could represent a therapeutic strategy to prevent neuronal cell death and improve outcomes of neurodegenerative diseases by promoting the degradation of tau.

1.5.4 DnaJC7

DnaJC7, also known as Tpr2, simultaneously binds Hsp70 and Hsp90 via its two TPR domains (72). To date, a link between DnaJC7 and tau has not been investigated. However, it is known that DnaJC7 plays an important role in steroid receptor chaperoning, as well as recycling substrates from Hsp90 back to Hsp70 via this unique TPR interaction

(72, 73). Additional studies are needed to understand if DnaJC7 regulates tau pathogenesis.

1.5.5 Tom34

Tom34 is a co-chaperone involved in mitochondrial protein import. One study found that in *Drosophila*, impaired Tom34 gene function led to enhanced tau pathology (67). Conversely, the same study demonstrated Tom34 overexpression was able to suppress tau toxicity elucidating a role for Tom34 in tau pathology in *Drosophila*. The mechanism by which Tom34 promotes tau pathology remains unclear. It is possible that mitochondrial dysfunction could lead to cellular stress which, in turn, could enhance tau pathology. Additional studies are needed to fully elucidate this interaction.

In addition, there are other TPR-containing Hsp90 co-chaperones such as UNC-45, Tom70, NASP, SGTA, SGTB, Cns1, CRN, Tah1, TPR1, DYX1C1, and AIPL1. However, very little is known about most of these co-chaperones in the brain and even less is known about their interactions with tau, therefore they will not be discussed in detail in this chapter.

1.6 Non-TPR co-chaperones

1.6.1 Cdc37

Cell division cycle 37 (Cdc37) slows the ATPase activity of Hsp90 allowing a prolonged interaction between Hsp90 and its client proteins (74). Cdc37 is also required for the stable folding of protein kinases in coordination with Hsp90 (75). Many of these kinases are known to phosphorylate tau at sites associated with AD, such as GSK3β and

MAPK13 (76, 77). Interestingly, overexpression of Cdc37 preserves tau, and its suppression reduces tau (78). However, additional studies are needed to better understand the dynamics between Cdc37 and tau phosphorylation.

1.6.2 p23

p23 has an opposing effect on Hsp90 compared to Aha1. p23 works by inhibiting the ATPase activity of Hsp90. The interaction between Hsp90 and p23 is nucleotide-dependent meaning that p23 can only interact with Hsp90 when ATP is bound (79). p23 works in a unique way to inhibit ATPase activity, it can either inhibit the hydrolysis process or it can impede the release of ADP and Pi (80). As a co-chaperone, p23 works to suppress protein aggregation and exhibits chaperoning activity, although p23 is not able to refold proteins on its own (81). Inhibition of p23 in an siRNA screen of Hsp90 co-chaperones showed that silencing p23 reduced both total and phospho-tau (66, 78). p23 also plays an important role in preventing endoplasmic reticulum (ER) stress-induced cell death, which can be triggered by misfolded proteins, like tau (82, 83). However, p23 can be cleaved during ER stress-induced cell death into a smaller p19 fragment which is then unable to exert its anti-apoptotic effects (84). A mutant p23 (p23D142N) that is uncleavable was shown to ameliorate the ER stress-induced cell death *in vitro* and suggests that this mutant p23 could be a potential therapeutic target in neurodegenerative diseases (84).

1.6.3 S100A1

S100 calcium-binding protein A1 (S100A1) interacts with Hsp90. One study used siRNA to screen several Hsp90 co-chaperones to investigate the effect on tau. This study

found that reductions in S100A1 also led to massive reductions in both phospho- and total tau levels in cells (66). S100A1 could play a role in stabilizing tau, thus leading to a worsening of tau pathology. Therefore, silencing or knocking down S100A1 could offer a potential therapeutic strategy for tauopathies.

1.6.4 FNIP1

The folliculin-interacting protein 1 (FNIP1) is able to interact with Hsp90 as a co-chaperone in order to inhibit its ATPase activity. One study found that FNIP1, in complex with FNIP2 and Hsp90, was able to stabilize the tumor suppressor folliculin (FLCN; (85)). FNIP1 was shown to interact directly with Hsp90, and it can also interact with other co-chaperones such as p23, Hop and Cdc37 (85). FNIP1 was also shown to compete for binding with Aha1 suggesting an important role for FNIP1 in the Hsp90 chaperone network (85). Additional studies are needed to determine if FNIP1 could regulate tau directly or potentially through competition with Aha1 to bind Hsp90 and alter its ATPase activity.

1.7 Aging in the Hsp90 Chaperone Network

All of the above mentioned co-chaperones interact with Hsp90 in order to form diverse heterocomplexes, however, changes in Hsp90 expression with aging can alter their composition. There is conflicting data on Hsp90 levels with age in both human and animal studies. One study focused on the basal levels of cytosolic Hsp90 in peripheral blood mononuclear cells (PBMC) and found that in aged human samples there was an increase in Hsp90 under normal physiological conditions when compared to young samples (86). Another study had similar findings in the hippocampus of aged gerbils. This

study demonstrated that cytosolic Hsp90 levels were significantly increased in the hippocampus of aged gerbils (24 months) compared to adult gerbils (6 months) (87). Conversely, there are also studies showing decreased levels of Hsp90 in aged human brain samples. For instance, two other studies investigated the levels of chaperone proteins in the human brain. One study found that cytosolic Hsp90 was repressed in the superior frontal gyrus, while another demonstrated a similar repression in the prefrontal cortex of aged patients compared to controls (21, 88, 89). Taken together, this data suggests that alterations in Hsp90 levels do not occur uniformly and that changes in the expression of Hsp90 with aging may vary between cell types and brain regions (88). While Hsp90 protein levels are an important factor with aging, co-chaperone expression levels could be equally important in heterocomplex formation.

In addition to the differences in expression levels of Hsp90, there are also changes in expression levels of co-chaperone proteins during the aging process. Almost all of the Hsp90 co-chaperones are repressed in aging, suggesting that these proteins could play important roles in maintaining homeostasis within the cell (21). For instance, CyP40, FKBP52, PP5, Hop, p23, and Aha1 are all repressed in the aged brain. All of these proteins are integral to the Hsp90 chaperone system and when levels of these proteins go down the Hsp90 chaperone network can no longer function normally, which can lead to an increased risk of developing a neurodegenerative disease. Interestingly, one co-chaperone is significantly induced in the aged brain and that is FKBP51. FKBP51 has several important roles within the cell including immunoregulation as well as helping with protein folding and trafficking in complex with Hsp90. Because FKBP51 is induced in aging, while many other co-chaperones are reduced, this suggests that the imbalance

seen in these proteins during aging could lead to completely different Hsp90 heterocomplexes resulting in the dysfunction of cellular homeostasis during aging.

Hsp90 is able to form many unique heterocomplexes with different co-chaperones in order to regulate protein triage. Hsp90 heterocomplexes are unique in that there is usually a specific progression of co-chaperones that interact with Hsp90 (10). One interesting aspect to these heterocomplexes is the fact that Hsp90 can bind multiple co-chaperones simultaneously. One study found that Hsp90 could form stable complexes with Hsp90, FKBP52, Hop, and p23 (43). There does appear to be a hierarchy though, with some co-chaperones able to bind more strongly than others. For example, Aha1 has been shown to compete with Hop, FNIP1, and p23 for the ability to bind with Hsp90 (42, 85). These competition dynamics between Aha1 and p23/FNIP1 suggest that there is a constant battle for control of the ATPase activity of Hsp90. Additionally, FKBP51 and FKBP52 have been shown to have greater relative binding to Hsp90 compared to other TPR co-chaperones (90). While not as strong as FKBP51 and FKBP52, PP5 forms more complexes with Hsp90 than most other TPR co-chaperones. Taken together, increased FKBP51 and decreased PP5 and CyP40 could contribute to an imbalance in Hsp90 heterocomplexes which may promote increased tau phosphorylation and aggregation causing neurotoxicity (20). This suggests an even more complex system in place because depending on the amount of certain co-chaperones and their relative ability to bind to Hsp90; certain maladaptive complexes could be more abundant than others with aging.

In addition to altering Hsp90 heterocomplex composition and client selection, altered Hsp90 co-chaperone expression can interfere with degradation of aberrant proteins via the proteasome or autophagy. As mentioned above, aged cells are often

inundated with misfolded and aggregated proteins, which can overload the Hsp90 chaperone network causing a negative spiral where there are not enough healthy chaperone molecules to refold or degrade aberrant proteins. In addition to the problems faced with an overwhelmed chaperone network, the proteolytic activity of the proteasome also declines with aging, and in fact Hsp90 has been shown to protect the proteasome from age-related, oxidative-dependent decline (91). However, with advanced aging, the association between Hsp90 and the proteasome drastically decreases (3). This suggests that because the Hsp90 chaperone system and the proteasome are so connected, when one starts to fail the other will fail as well leading to cytotoxicity and cell death. Proteins can also be degraded by CMA; however, CMA activity also decreases with age (92). Hsp90 and Hop are both involved in the CMA system; helping to unfold the target substrate before it can translocate into the lysosome for degradation. As mentioned previously, both Hsp90 and Hop are repressed in aging and therefore may not be able to assist in the translocation of substrates, leading to a buildup of misfolded or aggregated proteins. Post-translational modifications (PTMs) of Hsp90 can also complicate the matter further.

There are many different PTMs that can affect Hsp90 including phosphorylation, acetylation, S-nitrosylation, oxidation, and ubiquitination; and all of these PTMs can impact the chaperoning function of Hsp90. Phosphorylation of Hsp90 leads to reduced chaperoning ability and phosphorylation of specific tyrosine residues can affect the ability of Hsp90 to interact with distinct client proteins (93, 94). Acetylation of Hsp90 affects client protein interaction and also decreases binding of Hsp90 to ATP (93, 95). S-nitrosylation, oxidation and ubiquitination also inhibit Hsp90 chaperone activity (96–98). These PTMs

increase with aging and can alter the ability of Hsp90 to function properly as well as change the ability of different co-chaperones to bind. As the chaperone network declines with aging, so does the ability of the cell to recover from damaged proteins and stress, thus leading to an environment which promotes aberrant protein accumulation and neurotoxicity.

1.8 Targeting the Hsp90 Chaperone Network

Inhibition of the ATPase activity of Hsp90 has been shown to have positive outcomes in cell culture and animal models of tauopathy. Hsp90 ATPase inhibitors have been developed to target each of the three domains: N-terminal, middle, and C-terminal; with the majority of Hsp90 inhibitors targeting the N-terminal domain (99). Inhibition of Hsp90 induces the expression of protective chaperones, Hsp70 and Hsp40, further promoting the degradation of aberrant proteins (100). Previous studies have shown that Hsp90 inhibition decreased the levels of hyperphosphorylated and/or mutated tau species both in cells and mice. The Hsp90 N-terminal domain inhibitor, EC102, was used to demonstrate degradation of hyperphosphorylated pathologically relevant tau in cells (15). Another N-terminal Hsp90 ATPase inhibitor, 17-AAG, was shown to decrease levels of phosphorylated tau in cells, and a related N-terminal Hsp90 ATPase inhibitor, PU-DZ8, reduced soluble and insoluble tau in tauP301L mice (16). Although Hsp90 inhibitors have been in clinical development since 1999, none have reached New Drug Application (NDA) status (99). All of these clinical trials were focused on investigating Hsp90 inhibitors on various cancers. Hsp90 plays a similar role in both neurodegenerative disorders and cancer, however because of the complexity of the brain and the need for a blood-brain barrier (BBB) permeable drug, the clinical development of Hsp90 inhibitors for

neurodegenerative diseases has been even less successful. While the development of Hsp90 inhibitors is still underway, it is possible that the development of therapeutics which target Hsp90 heterocomplexes or discrete Hsp90 co-chaperones could open up additional avenues for success in developing a BBB-permeable drug.

In addition to offering more potential therapeutic targets, small molecules which modify Hsp90/co-chaperone interactions may also show more specificity for a specific pool of Hsp90 which may reduce the number of on-target side effects. There are very few Hsp90 co-chaperone targeting small molecules, and of these, only a handful of these have been investigated for their role in effecting tau. There is a Hop/Hsp90 complex specific inhibitor, C9, however, there is no available data on how chemical inhibition of this complex affects tau accumulation (101). The Cdc37/Hsp90 inhibitors, Celasterol and Withaferin A (102, 103), reduce tau levels and a new compound, platycodin D has just been discovered (104). Platycodin D does not affect the ATPase activity of Hsp90, but instead disrupts the interaction between Hsp90 and Cdc37 leading to client protein degradation without an increase in Hsp70 (104). More work still needs to be done to better understand the role of Cdc37 in tau phosphorylation to determine if targeting this complex is of therapeutic benefit. Developing drugs to target discrete FKBPs has been challenging due to their homology, however, despite their structural similarity they do display differences in conformational flexibility which could be a way to potentially target specific FKBPs in the future (105). Interestingly, one study demonstrated that patients chronically treated with FK506, which inhibits the PPIase domain of many of the FKBPs, significantly reduced the incidence of AD (106). The targeting FKBP51 is of great interest for the treatment of tauopathies as well as mood disorders (107). Recently a PPIase antagonist

has been developed which shows selectivity for FKBP51, but additional studies are needed to determine if targeting the PPIase domain of FKBP51 will be effective in regulating tau accumulation (53). There is one compound, MJC13, which targets the FKBP52-Hsp90-androgen receptor complex (108). MJC13 results in a reduced stress response which has demonstrated therapeutic potential in cancer, but so far MJC13 has not been investigated for a role in tau pathology (108). Additionally, Aha1-specific inhibitors have been recently developed (109). One of these inhibitors, KU-177, reduced insoluble tauP301L levels in cells (41). While this is an exciting result, more studies are needed to determine if Aha1 inhibitors regulate tau similarly *in vivo*. There is still much to be done to develop compounds which target the Hsp90 chaperone network, but there are a lot of promising leads which can be targeted to develop disease-modifying therapeutics.

1.9 Conclusions

The Hsp90 chaperone machinery plays a huge role in both aging and neurodegenerative diseases. Hsp90 is one of the most highly expressed proteins in the cell and is involved in a myriad of cellular processes. Previous work has focused on inhibition of Hsp90 to triage misfolded proteins. There are also many co-chaperones that associate with Hsp90 and play their own roles in aging and neurodegeneration. As these Hsp90 co-chaperones change with age they can significantly impact the propensity for certain neurodegenerative diseases. FKBP51 steadily increases with age and both FKBP51 and Aha1 are induced in the AD brain suggesting that these two co-chaperones negatively affect tau pathology. On the other hand, both CyP40 and PP5 are repressed in aged and AD brains. CyP40 disaggregates tau fibrils *in vitro* and PP5 dephosphorylates tau restoring microtubule binding, suggesting that increasing the levels or activity of these

co-chaperones could have a beneficial, neuroprotective role in diseases such as AD. These are just a few examples of how important maintaining the balance of Hsp90 co-chaperones is to homeostasis, and what can happen when they are altered in aging and disease. Hsp90 co-chaperones offer a unique target for potential therapeutics due to their specific roles within the Hsp90 machinery. Overall, more work needs to be done to develop BBB-permeable therapeutics to target discrete Hsp90 co-chaperones for the treatment of AD and other tauopathies.

Table 1.1 Summary of Hsp90 and Hsp90 co-chaperone levels in aging and Alzheimer's disease (AD). A summary of the levels of the Hsp90 chaperone network in both aging and AD human samples.

Chaperone	Gene	Function	Aging	AD	Reference
Hsp90α	*HSP90AA1*	Chaperone	Repressed	No Data	Brehme et al., 2014
Hsp90ß	*HSP90AB1*	Chaperone	Repressed	Repressed	Brehme et al., 2014
CyP40	*CYP40*	Peptidyl-prolyl isomerase	Repressed	Repressed	Brehme et al., 2014
FKBP51	*FKBP5*	Peptidyl-prolyl isomerase	Induced	Induced	Brehme et al., 2014; Blair et al., 2013
FKBP52	*FKBP4*	Peptidyl-prolyl isomerase	Repressed	Repressed	Brehme et al., 2014; Meduri et al., 2016
Xap2	*AIP*	Co-chaperone	Slightly Repressed	No Data	Brehme et al., 2014
PP5	*PPP5*	Ser/Thr phosphatase	Repressed	Activity repressed	Brehme et al., 2014; Liu et al., 2005
FKBP38	*FKBP8*	Peptidyl-prolyl isomerase	Unchanged	No Data	Brehme et al., 2014
FKBP36	*FKBP6*	Peptidyl-prolyl isomerase	Unchanged	No Data	Brehme et al., 2014
WISp39	*FKBPL*	Peptidyl-prolyl isomerase	Unchanged	Repressed	Brehme et al., 2014

Table 1.1, Continued

Hop	*STIP1*	Client protein maturation	Slightly Repressed	No Data	Brehme et al., 2014
CHIP	*STUB1*	E3 ubiquitin ligase	Unchanged	Unchanged	Brehme et al., 2014
DNAJC7	*DNAJC7*	Steroid receptor co-chaperone	Repressed	Repressed	Brehme et al., 2014
Tom34	*TOMM34*	Mitochondrial import protein	Unchanged	No Data	Brehme et al., 2014
UNC-45A	*UNC45A*	Myosin chaperone	Slightly Induced	Unchanged	Brehme et al., 2014
Tom70	*TOMM70*	Mitochondrial import protein	Repressed	Repressed	Brehme et al., 2014; Loerch et al., 2008
NASP	*NASP*	Co-chaperone	Slightly Induced	Induced	Brehme et al., 2014
SGTA	*SGTA*	Co-chaperone	Unchanged	No Data	Brehme et al., 2014
SGTB	*SGTB*	Co-chaperone	Repressed	Repressed	Brehme et al., 2014; Loerch et al., 2008
Cns1	*TTC4*	Co-chaperone	Induced	No Data	Brehme et al., 2014
CRN	*CRNKL1*	Co-chaperone	Slightly Repressed	No Data	Brehme et al., 2014
Tah1	*RPAP3*	RNA Polymerase II-associated protein	Repressed	No Data	Brehme et al., 2014
TPR1	*TTC1*	Co-chaperone	Unchanged	No Data	Brehme et al., 2014
DYX1C1	*DNAAF4*	Co-chaperone	Induced	No Data	Brehme et al., 2014
AIPL1	*AIPL1*	Co-chaperone	Unchanged	No Data	Brehme et al., 2014
Cdc37	*CDC37*	Inhibits ATPase activity	Unchanged	Repressed	Brehme et al., 2014
Aha1	*AHSA1*	Stimulates ATPase activity	Slightly Repressed	Induced	Brehme et al., 2014; Shelton et al., 2017
p23	*PTGES3*	Inhibits ATPase activity	Slightly Repressed	Unchanged	Brehme et al., 2014
S100A1	*S100A1*	Co-chaperone	No Data	No Data	
FNIP1	*FNIP1*	Co-chaperone	No Data	No Data	

Table 1.2 Summary of Hsp90 and Hsp90 co-chaperone knockout mice. This table contains information on the available knock-out mouse lines for the Hsp90 chaperone family.

	Protein	Gene	KO model	Viable	Phenotype	Reference
Hsp90	Hsp90α	*Hsp90aa1*	*Mouse*	Yes	Male mice, failure of spermatogenesis; viable and phenotypically normal into adulthood	Grad et al. PLoS One 2010
	Hsp90β	*Hsp90ab1*	*Mouse*	No	Early embryonic lethality (day E9)	Voss et al. Development 2000
TPR co-chaperones	Cyp40	*Cyp40*	*Mouse*	Yes	Phenotypically normal	Periyasamy et al. Oncogene 2010
	FKBP51	*Fkbp5*	*Mouse*	Yes	Resilliant to stress-induced depression-like behavior	Yong et al. JBC 2007; O'leary et al. PLoS One 2011; Touma et al. Biol Psychiatry 2011
	FKBP52	*Fkbp4*	*Mouse*	~50% are embryonic lethal	Reduced fertility in both males and females	Cheung-Flynn et al. Mol Endocrin 2005; Tranguch et al. PNAS 2005; Yang et al. Mol Endocrin 2006
	Xap2	*AIP*	*Mouse*	No	Embryonic lethality	Raitila et al. Am J Pathol 2010
	PP5	*Ppp5*	*Mouse*	Yes	Mice survive both embryonic development and into postnatal mice; defect in DNA damage checkpoint after ionizing radiation	Yong et al. JBC 2007
	FKBP38	*Fkbp8*	*Mouse*	No	Embryonically lethal	Bulgakov et al. Development 2004
	FKBP36	*Fkbp6*	*Mouse*	Yes	Both male and female mice are healthy and live normal lifespans; male mice are sterile	Crackower et al. Science 2003
	WISp39	*Fkbpl*	*Mouse*	No	Heterozygous FKBPL mice appear normal	Yakkundi et al. Arterioscler Thromb Vasc Biol 2015
	Hop	*Stip1*	*Mouse*	No	Embryonically lethal around day E9.5-10.5	Beraldo et al FASEB J 2013
	CHIP	*Stub1*	*Mouse*	Yes	Develop normally but are susceptible to stress-induced apoptosis of multiple organs; increased peri- and postnatal lethality	Dai et al. EMBO J 2003

Table 1.2, Continued

	DnaJC7	*Dnajc7*	*Mouse*	Yes	No information on phenotype	Dickinson et al. Nature 2016
	Tom34	*TOMM34*	*Mouse*	Yes	Phenotypically normal	Terada et al. J Biochem 2003
	UNC-45A	*UNC45A*	*Mouse*	No	Embryonic lethality	Dickinson et al. Nature 2016
	Tom70	*TOMM70*	*No*	N/A		
	NASP	*NASP*	*Mouse*	No	Embryonic lethality	Richardson et al. JBC 2006
	SGTA	*SGTA*	*Mouse*	Yes	Less fertile with small liters and higher neonatal death rates; smaller body size in both males and females	Philp et al. Nature Scientific Reports 2016
	SGTB	*SGTB*	*No*	N/A		
	Cns1	*TTC4*	*Mouse*	Yes	Phenotypically normal	Josefowicz et al. Nature 2012
	CRN	*CRNKL1*	*No*	N/A		
	Tah1	*RPAP3*	*No*	N/A		
	TPR1	*TTC1*	*No*	N/A		
	DYX1C1	*DYX1C1*	*Mouse*	Yes	Embryonic lethality in approx. 2/3; surviving mice develop severe hydrocephalus by postnatal day 16 and died by P21	Tarkar et al. Nat Genetics 2013
	AIPL1	*AIPL1*	*Mouse*	Yes	Phenotypically normal	Ramamurthy et al. PNAS 2003
Non TPR co-chaperones	Cdc37	*Cdc37*	*C. elegan*	No	Embryonically lethal in C. elegans	Beers & Kemphues, Development 2006
	Aha1	*Ahsa1*	*Mouse*	Yes	No information on phenotype	The Jackson Laboratory: Stock No: 029805
	p23	*Ptges3*	*Mouse*	No	Perinatal lethality resulting from defective lung development; Abnormal skin and reduced expression of GR markers	Grad et al. Mol and Cell Biol 2006; Lovgren et al. Mol and Cell Biol 2007; Nakatani et al. Biochem and Biophys Res Comm 2007
	S100A1	*S100A1*	*Mouse*	Yes	Phenotypically normal	Jun Du et al. Mol Cell Biol 2002
	FNIP1	*FNIP1*	*Mouse*	Yes	Phenotypically normal	Hasumi et al. PNAS 2015

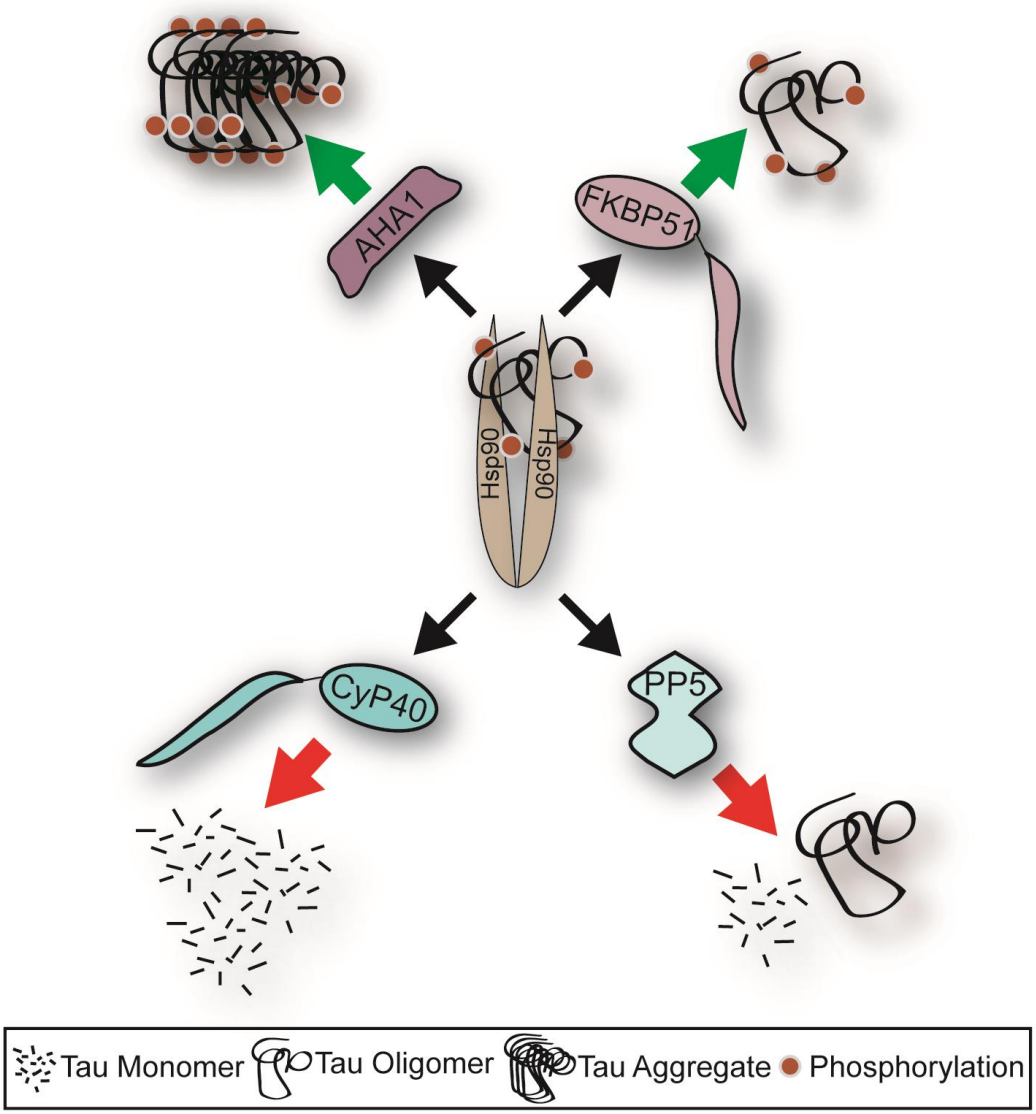

Figure 1.1. Schematic depicting fate of tau following Hsp90 interaction with distinct co-chaperones; the impact of Alzheimer's disease on the levels of co-chaperones. Aha1 and FKBP51 protein levels are induced in AD, and their association to tau leads to increased aggregation. Whereas, CyP40 and PP5 levels are repressed in AD, and their association to tau leads to reduced tau aggregation. This schematic highlights the important role of co-chaperones in AD.

Chapter Two[1]:

The Hsp90 activator Aha1 drives production of tau aggregates

2.1 Abstract

The microtubule-associated protein tau forms neurotoxic aggregates that promote cognitive deficits in tauopathies, the most common of which is Alzheimer's disease (AD). The 90-kDa heat shock protein (Hsp90) chaperone system affects the accumulation of these toxic tau species, which can be modulated with Hsp90 inhibitors. However, many Hsp90 inhibitors are not blood-brain barrier permeable and several present associated toxicities. Here, we find that the co-chaperone, activator of Hsp90 ATPase homolog 1 (Aha1), dramatically increased the production of aggregated tau. We see that Aha1 overexpression in an iHek-P301L tau model led to the accumulation of insoluble tau. Whereas, treatment with a novel Aha1 inhibitor, KU-177, dramatically reduced the accumulation of insoluble tau. Overall, these data demonstrate that Aha1 contributes to tau fibril formation through Hsp90. This suggests that therapeutics targeting Aha1 may reduce toxic tau species, which could be beneficial in slowing or preventing the progression of tauopathies.

---

[1]Portions of this work were previously published (Shelton LB et al., 2017) and are used with permission of the publisher.

2.2 Introduction

The microtubule associated protein tau (MAPT, tau) accumulates and aggregates in a family of neurodegenerative diseases called tauopathies (110), the most common being Alzheimer's disease (111). In particular, the pathogenic formation of oligomeric tau species is thought to be a major contributor to disease progression (112). One study has shown that injection of recombinant full-length human tau oligomers *in vivo* led to synaptic dysfunction and impaired memory, whereas injection of tau fibrils and monomers did not (113). Therefore strategies aimed at reducing oligomeric tau accumulation could hold therapeutic promise for these diseases (114).

Molecular chaperones, including the 90-kDa heat shock protein (Hsp90), regulate protein folding, degradation, and accumulation (115). Of the proteins regulated by Hsp90, often referred to as 'clients,' tau is one of the most thoroughly characterized (116). In the past decade, Hsp90 emerged as one of the next breakthrough drug targets for diseases of aging, particularly for neurodegenerative diseases like tauopathies (117). Small molecules inhibiting the ATPase activity of Hsp90 showed great promise in preclinical models, prompting the development of a host of clinical leads (118), but the translation of this pre-clinical success into patients has been disappointing. Not only have many leads suffered from poor blood-brain barrier permeability (119), but toxicity has also dampened enthusiasm (120, 121). This has led to the pursuit of Hsp90 co-chaperones as distinct drug targets offering an alternative to Hsp90 (115, 122).

Activator of Hsp90 ATPase homolog 1 (Aha1) is the only one of these co-chaperones known to stimulate Hsp90 ATPase activity (123). This small 38kDa co-

chaperone binds to the N-terminal and mid-domains of Hsp90, inducing a partially closed conformation that accelerates the progression of the ATPase cycle dramatically (123, 124). Therefore, small molecules targeting the interaction of Hsp90 with Aha1 could be beneficial in disease by reducing Hsp90 ATPase activity (125, 126). Here we sought to determine if Aha1 could facilitate the pathogenesis of tau by stimulating Hsp90 activity. We determined that Aha1 stimulation of Hsp90 activity can drive tau fibril formation, *in vitro*. Moreover, inhibiting the interaction between Aha1 and Hsp90, using a small molecule, reduced recombinant tau fibril formation as well as insoluble tau accumulation in cultured cells. Our findings suggest that targeting Hsp90 co-chaperones may enable inhibition of tau aggregation, which could re-energize the translational appeal of the Hsp90 chaperone network as a drug target.

2.3 Materials and Methods

2.3.1 Antibodies

The following antibodies were used: Anti-Aha1 antibodies (StressMarq, SMC-172D and Abcam, ab83036 for IP), anti-Hsp90 α (StressMarq, SMC-149B), anti-GAPDH (Proteintech, 60004-1-Ig), H-150 anti-tau (Santa Cruz Biotechnology, sc-5587), and anti-tau pT231 (Anaspec, 55313-025). PHF1 anti-tau (pS396/404) was a kind gift from Dr. Peter Davies.

2.3.2 Plasmids and viral vectors

Aha1 WT and Aha1 E67K expression plasmids were generated in our lab using the pCMV6 backbone.

2.3.3 Protein expression

Recombinant human P301L tau, Aha1, Aha1 E67K, p23, FKBP51, FKBP52 and CDC37 were cloned into bacterial expression vector, pet28a with a His tag followed by a TEV sequence. Plasmids were transformed into *E.coli* (BL21) one-shot star cells and plated onto kanamycin-agar plates. Plates were grown at 37°C for approximately 16 hours. 10mL LB broth with kanamycin starter cultures were then inoculated with a colony and the starter culture grown for 8 hours. 1L cultures were then inoculated at 1:100 dilution and grown to OD600 of 0.8. Cultures were induced with the addition of 1mM IPTG and the incubator temperature was reduced to 16°C. Cultures were then grown for 14 hours. Cells were then pelleted at 3,500 x *g* for 30 minutes and supernatant discarded. Pellets were resuspended in lysis buffer (20 mM Tris-HCl pH 8.0, 500 mM NaCl, 10 mM Imidazole with protease inhibitors) and frozen at -80°C. Bacterial pellets were then thawed and lysed by sonication. Lysates were then spun at 50,000 x *g* for 1 hr. Next, the supernatant was purified by nickel affinity chromatography (Nickel Resin, Fisher #PI88222). Protein purity and expression was then checked by Coomassie stained SDS-PAGE. Next, the protein was digested with TEV protease, removing the His tag. Finally, proteins were purified by a size exclusion column (HiLoad 16/600 Superdex200pg). Proteins were then stored at -80°C. Hsp90α protein was a kind gift from Dr. Johannes Buchner.

2.3.4 Transmission Electron Microscopy

10 µL of protein samples were adsorbed onto square mesh copper grids (EMS300-Cu) for 60 seconds, washed twice with 10 µL of deionized water and excess water removed by wicking with filter paper. Samples were negatively stained with 1% uranyl acetate for

30 seconds and dried overnight. Grids were viewed using a JEOL 1400 Digital Transmission Electron Microscope and images were captured with a Gatan Orius wide-field camera. Fields shown are representative.

2.3.5 Thioflavin T fluorescence assay

10 µM P301L tau was incubated with 400 nM of the indicated chaperone in 100 µM Sodium Acetate pH 7.0 buffer with 2mM DTT, 2.5uM heparin (3,000 Da), and 10uM Thioflavin ThT in 100 µL volumes in a 96-well black clear-bottom plate (Fisher #07-200-525) for 3 days at 37°C. Fluorescence was read at 440 nm excitation and 482 nm emission in a BioTek Synergy H1 plate reader at indicated time points. All conditions were performed at least in duplicate.

2.3.6 Cell culture and transfection

iHek-P301L cells (32) and luciferase expressing PC3-MM2 cells (127) were cultured in DMEM media supplemented with 10% FBS and 1% Penicillin-Streptomycin (Invitrogen). Inducible cells were incubated with 3 µg of tetracycline for 72 h. 48 h prior to harvest, transfections were performed with 2.5 µL Lipofectamine 2000 (Invitrogen) per 1 µg of DNA, which was incubated in serum-free Opti-MEM for 5 minutes before adding the mixture dropwise to the cells. KU-177 was added 24 h prior to harvest at indicated concentrations. Cells were harvested in Hsaio TBS buffer (50mM Tris Base, 274mM NaCl, 5mM KCl, pH 8.0) containing protease inhibitors. Samples were prepared as previously described (128) to obtain soluble (S1) and Sarkosyl-insoluble (P3) fractions.

2.3.7 Co-immunoprecipitation

Co-immunoprecipitation of Hsp90α with Aha1 from PC3- MM2 and iHek P301L cells incubated with the indicated compounds for 24 hours were performed as previously described (129).

2.3.8 Luciferase refolding assay

Compound dissolved in DMSO at the indicated concentrations or a DMSO control was evaluated in a luciferase refolding assay in PC3-MM2 cells as previously described (130) and dose–response curves of the luminescence signal relative to DMSO control were generated using GraphPad Prism 5.0.

2.3.9 Western blot and dot blot analysis

Cell samples were analyzed by Western blot using 4-15% SDS gradient gels (BioRad). Antibody dilutions were 1:1000 unless otherwise stated, and all secondary antibodies were used at 1:1000 (Southern Biotech). Blots were developed using ECL (Pierce) on a LAS-4000 mini imager (GE Healthcare).

2.3.10 Statistical analysis

To compare two groups, a t-test was used. Groups larger than two were evaluated using a one-way ANOVA with Dunnett's multiple comparison test. P values below 0.05 were considered significant.

2.4 Results

2.4.1 Aha1 enhances Hsp90-dependent tau aggregation.

Since Hsp90 has been shown to exacerbate tau fibril formation (131), we screened five established Hsp90 co-chaperones to determine whether they had an inhibitory or stimulatory effect on this process. Recombinant P301L tau was incubated with Hsp90 in the presence of ATP with or without co-chaperone proteins, as indicated (Fig. 2.1A). Aha1 was the only co-chaperone to show a significant enhancement of tau fibril formation; while CDC37, p23, FKBP51 and FKBP52 were not significantly different than Hsp90 alone. We then examined the effects of Hsp90 and Aha1 on tau fibril formation over time. We found the most potent inducer of tau fibril formation was Hsp90 and Aha1 combined (Fig. 2.1B). Moreover, Aha1 alone did not affect tau aggregation. These results were also confirmed using transmission electron microscopy (TEM), which shows an increase in tau fibrils in the presence of Hsp90, and an exacerbation of fibrils when both Hsp90 and Aha1 are present (Fig. 2.1C); suggesting that Aha1 could be responsible for the enhancement of tau aggregates seen. Additionally, a mutant Aha1-E67K, which does not bind to Hsp90 (Fig. 2.2A), did not enhance tau fibril formation (Fig. 2.1D). Since heparin is a known tau aggregation inducer, and tau aggregation can be modulated by DTT, we conducted control experiments to check if the aggregation behavior of tau can be affected by Hsp90, Aha1, or their combination in the absence of heparin or DTT. Tau did not fibrillate under these conditions within the timeframe examined (Fig. 2.3A and B). Moreover, since Aha1 is a known stimulator of Hsp90 ATPase activity (123, 124), next, we also investigated the effects of these proteins on tau aggregation in the absence of ATP. We found that ATP was essential

for Aha1/Hsp90-mediated tau aggregation (Fig. 2.1E). Together, these data indicate that Aha1 utilizes ATP to enhance Hsp90-mediated tau aggregation.

2.4.2 KU-177 inhibits interaction between Hsp90 and Aha1.

There are no commercially available Aha1-specific inhibitors. We received novobiocin analogs from Dr. Brian Blagg which were designed to bind to both Hsp90 and Aha1 (KU-174) or to only Aha1 (KU-177, KU-308) (Fig. 2.4A). Immunoprecipitation of Aha1 from PC3-MM2 cells revealed that Aha1 and Hsp90 complexes were inhibited by KU-308, KU-177, and KU-174 (Fig. 2.4B). Hsp90-mediated refolding of denatured luciferase was inhibited with KU-174 (Fig. 2.4C), indicating that this compound directly inhibits Hsp90, consistent with a previous report (129). However, both KU-308 and KU-177, which lack the noviose sugar required for Hsp90 binding (Fig 2.4A, red), did not inhibit luciferase refolding (Fig. 2.4C). This suggests that these compounds do not directly inhibit Hsp90, as they were engineered to specifically bind to Aha1. Because of these characteristics, we chose to use KU-177 as our lead compound. We further tested the ability of KU-177 to inhibit the interaction between Hsp90 and Aha1 in HEK cells. Consistent with the PC3-MM2 cells, immunoprecipitation of Aha1 revealed that KU-177 inhibited the binding of Aha1 to Hsp90 (Fig. 2.4D).

2.4.3 KU-177 inhibits tau aggregation in vitro.

We investigated the ability of KU-177 to inhibit Aha1-mediated tau aggregation. Recombinant P301L tau was incubated with Hsp90 alone or Hsp90 and Aha1, then treated with KU-177 or DMSO as a control. KU-177 was able to significantly reduce tau fibril formation compared to the DMSO control (Fig. 2.5A). KU-177 showed a robust

reduction in tau fibril formation, as observed by TEM (Fig. 2.5B). iHEK-P301L cells transfected with Aha1-WT or Aha1-E67K were treated with KU-177 and harvested to examine soluble and Sarkosyl-insoluble tau. We see that both the mutant Aha1-E67K as well as the Aha1 inhibitor KU-177 were able to reduce insoluble tau (Fig. 2.5C). We also noted that KU-177 increased soluble, phosphorylated tau however, this finding was not significant.

2.5 Discussion

In this study we identified the Hsp90 co-chaperone, Aha1, as a potential therapeutic target for the treatment of tauopathies. Our data suggest that Aha1 increased tau fibril formation resulting in insoluble tau accumulation by stimulating Hsp90 ATPase activity. Additionally, we demonstrated that the novel Aha1 inhibitor, KU-177, reduced the accumulation of insoluble P301L tau in cultured cells. This suggests that Aha1 may be a promising target for the development of therapeutics directed toward reducing tau aggregation.

Previous work has focused on Hsp90 as a therapeutic target in order to reduce the toxic load of amyloidogenic proteins in cells (132). However, this endeavor has been challenging as Hsp90 has many client proteins within the cell and inhibiting this chaperone can lead to many pleiotropic effects (120, 133). Compounds that target specific Hsp90 co-chaperones (122) are being investigated for their potential to be less toxic as well as more specific (115). Targeting the Hsp90/p23 and Hsp90/CDC37 complexes with celastrol analogs (134–137) or withanolides (138–140) has been

investigated. However, these compounds still bind Hsp90 and have effects similar to Hsp90 inhibitors (140, 141). Alternatively, small molecule inhibitors of Hsp90/HOP complexes disrupt this complex by binding directly to HOP (142). One of these compounds, C9, was shown to have anticancer effects similar to direct Hsp90 inhibition, without inducing heat shock response (101). Until recently, there were no known small molecule inhibitors of Aha1. Ghosh and colleagues identified compounds which bind to either Hsp90 or Aha1 based on the novobiocin scaffold (129). More recently, two additional Aha1/Hsp90 inhibitors were identified (143). These compounds demonstrated protection against pathologies related to cystic fibrosis, but it is still unclear if these inhibitors bind directly to Hsp90 or Aha1.

Here, we demonstrated that the Aha1-binding inhibitor, KU-177, reduced Hsp90/Aha1-mediated toxic tau accumulation. Further studies will be required to determine the pharmacokinetics, brain distribution, and efficacy of KU-177 and future classes of Aha1 inhibitors. Exploring Aha1 as an alternative to Hsp90 inhibition could re-energize the field, as Aha1 can be targeted more specifically and perhaps avoid the potential negative side effects that are seen when Hsp90 is inhibited. Additional studies are also needed to determine the *in vivo* relevance of this work. Future studies could investigate the effect of Aha1 knock-down on tau pathology *in vivo*. Collectively, this study identified a role for Aha1 in the progression of tauopathies. This suggests inhibition of Aha1 may prevent the accumulation of pathogenic tau.

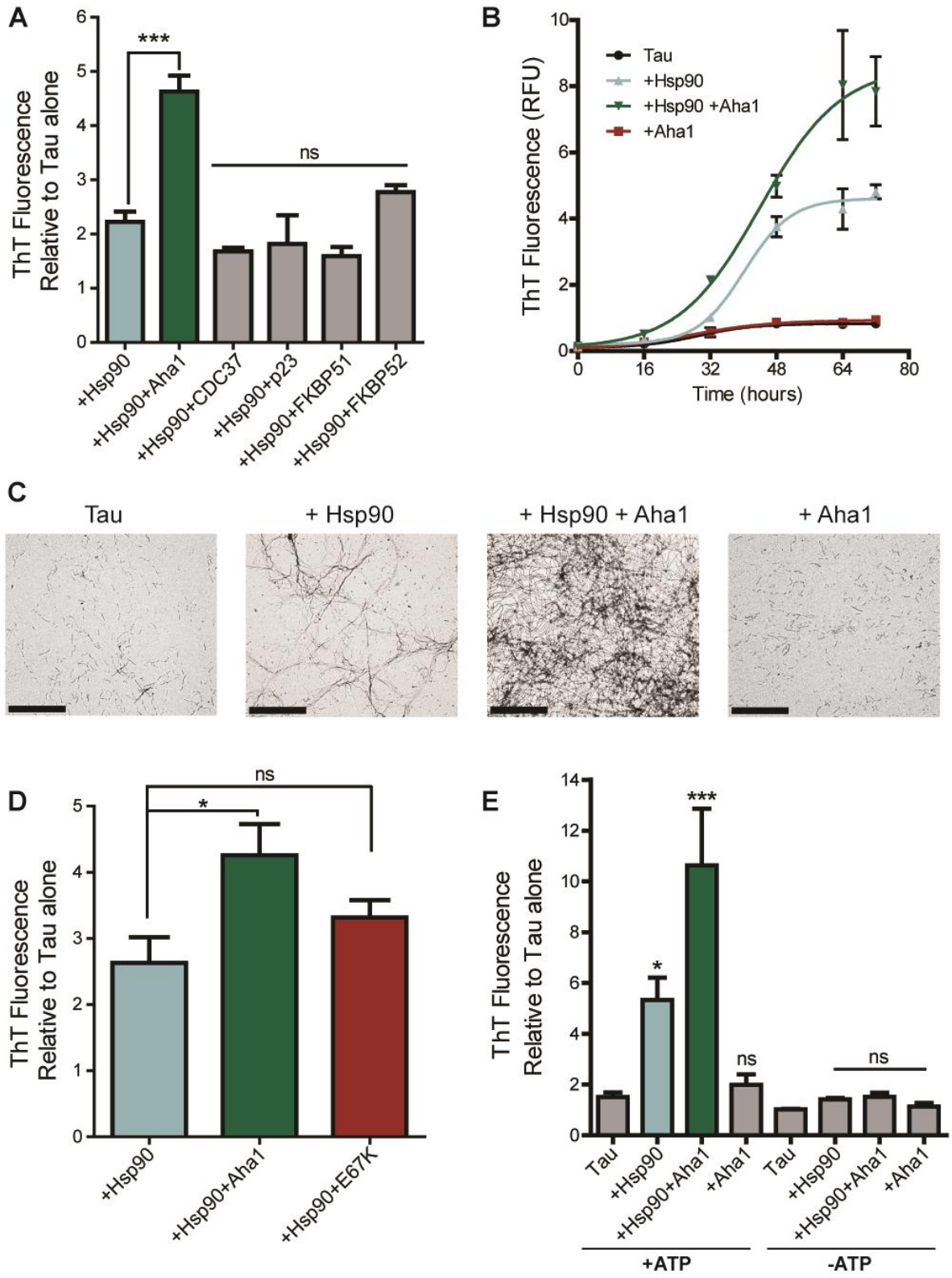
A
ThT Fluorescence Relative to Tau alone
***
ns
+Hsp90
+Hsp90+Aha1
+Hsp90+CDC37
+Hsp90+p23
+Hsp90+FKBP51
+Hsp90+FKBP52
B
ThT Fluorescence (RFU)
Tau
+Hsp90
+Hsp90 +Aha1
+Aha1
Time (hours)
C
Tau
+ Hsp90
+ Hsp90 + Aha1
+ Aha1
D
ThT Fluorescence Relative to Tau alone
ns
*
+Hsp90
+Hsp90+Aha1
+Hsp90+E67K
E
ThT Fluorescence Relative to Tau alone
*
***
ns
ns
Tau
+Hsp90
+Hsp90+Aha1
+Aha1
+ATP
-ATP

Figure 2.1. Hsp90 and Aha1 synergize to form tau aggregates. (A) Recombinant P301L tau fibril formation measured by ThT fluorescence, comparing the effect of 5 different recombinant co-chaperone proteins with Hsp90 and ATP (Results represent the mean ± SEM, n=3; *** = $p < 0.001$). (B) Recombinant P301L tau fibril formation measured by ThT fluorescence over a period of 72 hr with or without the addition of Hsp90 and Aha1 (Results represent the mean ± SEM, n=3). (C) Representative 20,000x TEM images of recombinant P301L tau fibrils formed in the presence of indicated chaperone proteins with ATP, scale bar represents 2 µm. (D) Recombinant P301L tau fibril formation was measured by ThT fluorescence in the presence ATP and chaperones as indicated (Results represent the mean ± SEM, n=3; * = $p<0.05$). (E) Recombinant P301L tau fibril formation measured by ThT fluorescence with varying mixtures of Hsp90, Aha1 and ATP as indicated (Results represent the mean ± SEM, n=3; *** = $p < 0.001$, *$p<0.05$).

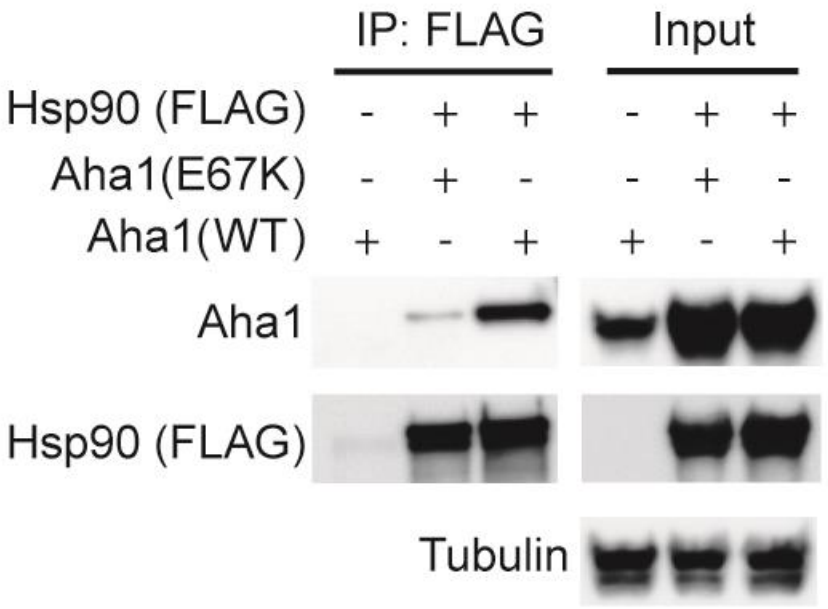

Figure 2.2. **E67K-Aha1 mutation reduces tau aggregation *in vitro***. (A) Western blot of immunoprecipitated Hsp90 (FLAG) from iHek cells transfected with either Aha1-WT or Aha1-E67K.

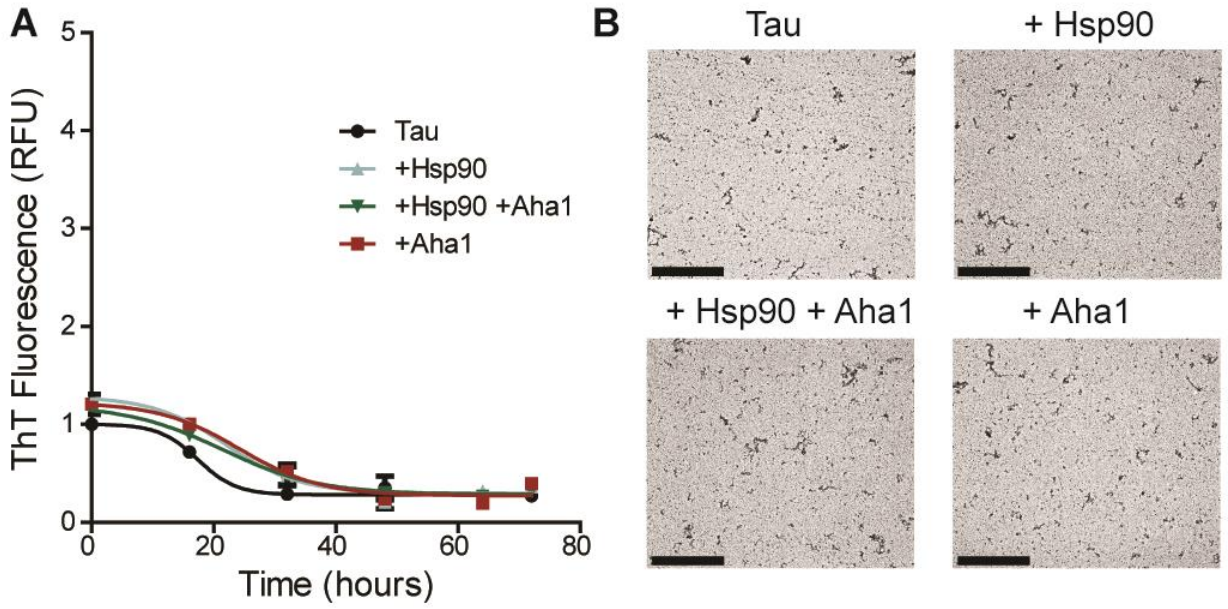

Figure 2.3 Tau fibril formation without heparin and DTT. (A) Recombinant P301L tau fibril formation measured by ThT fluorescence over a period of 72 hr with or without the addition of Hsp90 and Aha1 (Results represent the mean ± SEM, n=3). (B) Representative 20,000x TEM images, scale bar represents 2 µm.

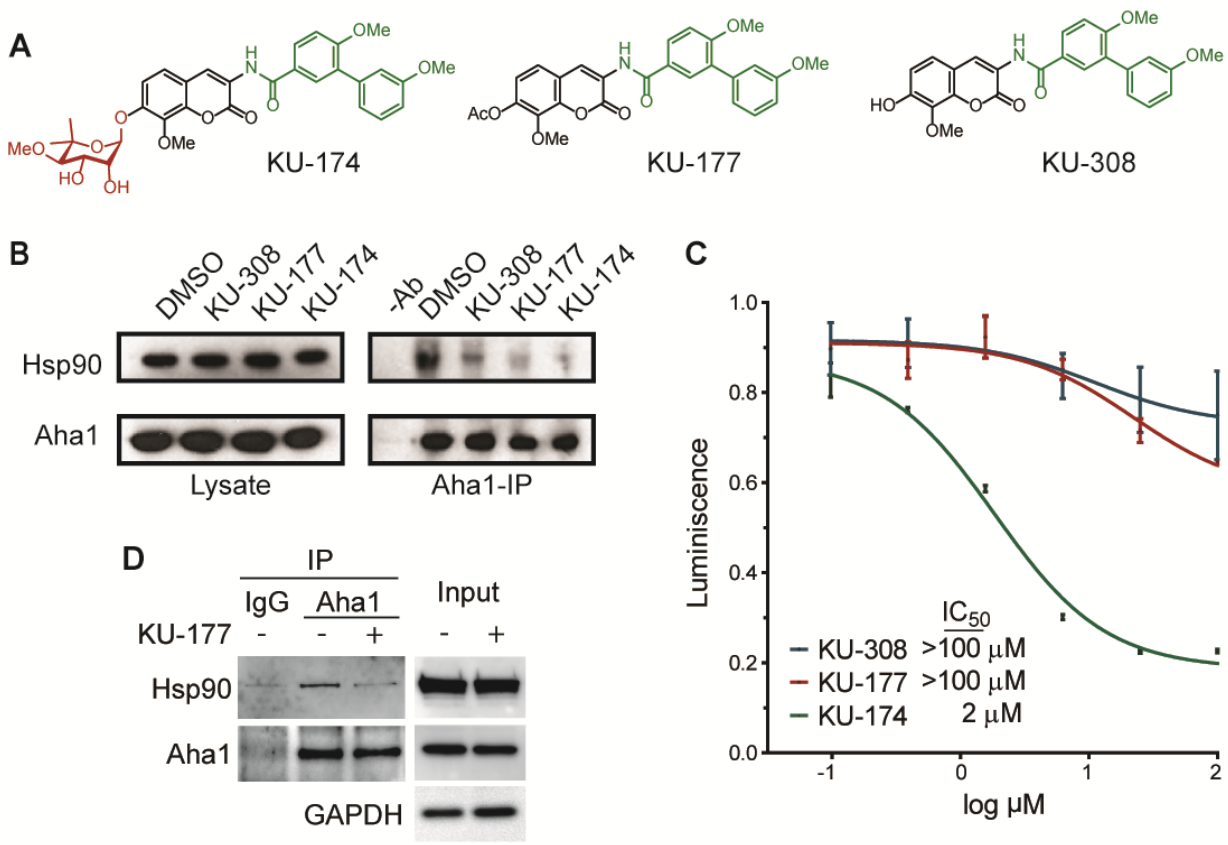

Figure 2.4. KU-177 inhibits interaction between Hsp90 and Aha1. (A) Chemical structure of the novobiocin analogs KU-174, KU-177 and KU-308. The noviose sugar moiety (red) is required for Hsp90-binding of novobiocin analogs and is absent in KU-177 and KU-308. The biaryl amide moiety (green) has been shown to interact with Aha1 (18). (B) Immunoprecipitated Aha1 from PC3-MM2 cells treated with ± 10 μM KU-308, KU-177 or KU-174 for 24 hours were analyzed by Western blot. Without antibody (-Ab) indicates a mock immunoprecipitation. (C) Comparison of Hsp90–mediated luciferase refolding activity in PC3-MM2 cell treated with DMSO or 100, 25, 6.25, 1.56, 0.39, and 0.097 μM KU-308, KU-177 or KU-174 for 2 hours. IC_{50} value for KU-177 is shown (R^2 = 0.98). Dose response curves for KU-308 and KU-177 suggest the IC_{50} values would be higher than the range of concentrations examined here. (KU-308, KU-174 n=3; KU-177

n=2). (D) Immunoprecipitated Aha1 from iHEK cells treated ± 10 μM KU-177 for 24 hours were analyzed by Western blot.

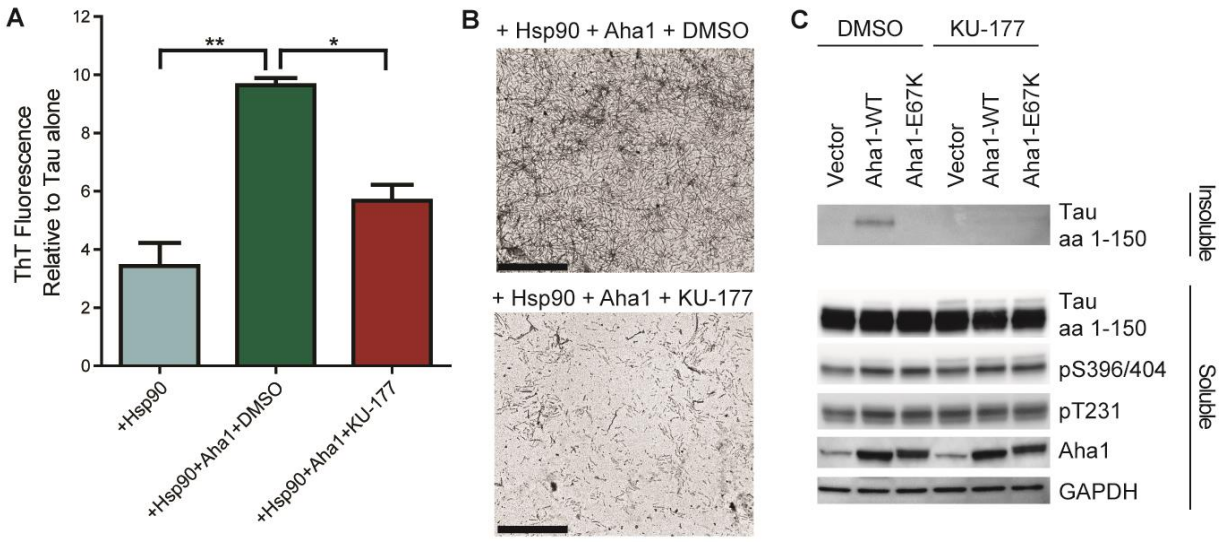

Figure 2.5. KU-177 inhibits Aha1 enhancement of Hsp90-mediated tau aggregation. (A) Recombinant P301L tau fibril formation measured by ThT fluorescence, comparing the effect of 10 µM KU-177 or DMSO on tau fibril formation (Results represent the mean ± SEM, n=3; ** = $p < 0.01$, * = $p < 0.05$). (B) Representative 20,000x TEM images of recombinant P301L tau fibrils formed in with KU-177 or DMSO control, scale bar represents 2 µm. (C) iHek P301L cells transfected with Aha1-WT, Aha1-E67K or empty vector were treated with 10 µM KU-177 or DMSO then harvested and soluble and Sarkosyl-insoluble fractions were prepared. Blots were probed by antibodies as indicated.

Chapter Three[1]:

Overexpression of Aha1 accelerates tau pathology and neurotoxicity in rTg4510 mice

3.1 Abstract

Pathological tau aggregates are the hallmark of a group of diseases deemed tauopathies. Several forms of tau can be seen within the brain, such as tau monomers, oligomers, and fibrils, with tau oligomers thought to be the most toxic. We previously demonstrated that Hsp90, together with Aha1, can significantly increase the production of aggregated tau species *in vitro*. However, the impact of Hsp90/Aha1 interaction on tau *in vivo* has not yet been investigated. Therefore, this study sought to investigate the effects of Aha1 overexpression in the rTg4510 mouse model of tauopathy. We found that Aha1 overexpression led to an increased production of both insoluble and oligomeric tau species in the hippocampi of the mice. Significant cognitive deficits and neuronal loss was also seen in mice overexpressing Aha1. This suggests that Aha1 overexpression can induce the formation of pathological tau aggregates. This work provides precedent for the use of Aha1 as a novel therapeutic target for the treatment of tauopathies.

---

[1]Portions of this work were previously published (Shelton LB et al., 2017) and are used with permission of the publisher.

3.2 Introduction

Tau, a microtubule associated protein, accumulates in many diseases known as tauopathies, the most common being Alzheimer's disease (AD). Hyperphosphorylation of tau allows it to disassociate from the microtubule and leads to its propensity to aggregate (144). It has been assumed for many years that neurofibrillary tangles (NFTs) were the cause of toxicity because they correlate well with disease progression (145). However, more recent evidence suggests that tau oligomers may be the toxic form of tau in neurodegenerative disease (145). It is plausible that multiple tau conformations can cause toxicity, but tau oligomers appear to be the most toxic species of tau.

There are several key mutations that occur in tauopathies, which lead to tau becoming more easily abnormally hyperphosphorylated, including G272V, P301L, V337M and R406W (146). There are several mouse models that use these mutations to mimic tauopathies, and to some extent, AD. The P301L mutation has been used to generate the greatest number of transgenic mouse lines (147). The first mouse line expressing the P301L mutation was the JNPL3 mice, with 4R/0N (four-repeat, no amino-terminal inserts) under the control of the mouse prion promoter (147, 148). While this mouse line did develop neurofibrillary tangles in the diencephalon, brainstem and cerebellar nuclei, there were no clear cognitive deficits or neuronal loss and these mice had a severe motor impairment (147). Since then, many other mouse lines have been created expressing the P301L mutation.

The rTg4510 mouse line is another transgenic mouse that expresses the P301L mutation. Expression of the transgene is driven by a forebrain specific Ca^{2+} calmodulin

kinase II promoter system that results in high levels of expression in the hippocampus and neocortex (128). An interesting aspect of this mouse line is that transgene expression is induced via the tetracycline-operon responsive element allowing suppression after treatment with doxycycline (128). The pathological hallmarks of this mouse model are striking with an age-dependent accumulation of neurofibrillary tangles (NFT), which can be seen as early as 2.5 months of age, as well as Sarkosyl-insoluble tau (128, 149). Additionally, massive neuronal loss can be seen, reaching over 80% loss in the CA1 of the hippocampus and dentate gyrus by 8.5 months of age (149). Due to this massive neuronal loss, the rTg4510 mice also display impaired cognition in spatial learning and memory tasks (128, 150). Astoundingly, tau suppression via doxycycline administration is able to reverse the cognitive deficits seen, even after accumulation of pathological NFTs and neuronal loss has occurred (150). Previous work from our lab, has focused on using co-chaperones, proteins that assist chaperones in protein folding and other functions, to modulate tau pathology in the rTg4510 mice. FKBP51 and CyP40, while both immunophilins, have very different effects on tau pathology (49, 131). While FKBP51 increases oligomeric tau and enhanced neurotoxicity, CyP40 had the opposite effect (49, 131). These studies demonstrate that co-chaperones can have different effects on tau aggregation and provide a precedent for examining the role of Aha1 in this mouse model. Additionally, Aha1 is the only known stimulator of the ATPase activity of Hsp90, providing a unique co-chaperone target that, if inhibited, could mimic the effects seen from Hsp90 inhibition (41, 123). Hsp90 inhibition has previously been shown to modulate tau pathology, however, due to toxicity and bioavailability, Hsp90 inhibitors have not been successful in clinical populations (15, 18, 19). Therefore, finding a co-chaperone that can

also modulate tau pathology with more specificity could provide additional therapeutic targets for the treatment of tauopathies.

For these reasons, we chose to examine the effects of overexpression of Aha1 in the rTg4510 mouse model. Aha1 was found to be co-localized with tau tangles in AD brain samples, suggesting that it is a clinically relevant co-chaperone. We also found that Aha1 overexpression increased both oligomeric and Sarkosyl-insoluble tau in the hippocampi of the mice. Additionally, we saw increased neuronal loss and cognitive deficits in mice overexpressing Aha1. Our findings suggest that overexpression of Aha1 in a mouse model of tauopathy significantly worsens the phenotype seen in these mice.

3.3 Materials and Methods

3.3.1 Antibodies

The following antibodies were used: Anti-Aha1 antibodies (StressMarq, SMC-172D and Abcam, ab83036 for IP), anti-Hsp90 α (StressMarq, SMC-149B), anti-GAPDH (Proteintech, 60004-1-Ig), anti-NeuN (Millipore, MAB377B), H-150 anti-tau (Santa Cruz Biotechnology, sc-5587), and anti-tau pT231 (Anaspec, 55313-025). PHF1 anti-tau (pS396/404) was a kind gift from Dr. Peter Davies. T22 anti-tau oligomer was a kind gift from Dr. Rakez Kayed.

3.3.2 Plasmids and viral vectors

The Aha1 expression plasmid was generated in our lab using the pCMV6 backbone. Adeno-associated virus (AAV) serotype 9-Aha1 and AAV9-mCherry were generated in our lab for murine gene therapy studies.

3.3.3 Human tissue processing

Brain tissue samples from the medial temporal gyrus of patients with Braak stages 2, 5 or 6 were provided by the University of California Alzheimer's Disease Research Center (UCI-ADRC) and the Institute for Memory Impairments and Neurological Disorders. Samples were fixed in 4% paraformaldehyde overnight, then sucrose gradients up to 30% were used and tissue was sectioned on a sliding microtome at 25 µm thick sections. Sections were stored at 4ºC in Dulbecco's phosphate buffered saline (PBS) supplemented with 0.065% sodium azide until they were used for immunohistochemistry.

3.3.4 Animal studies and tissue processing

rTg4510 (Jackson labs) and non-transgenic control mice received bilateral stereotaxic hippocampal (X = ±3.6, Y = -3.5, Z = +2.68) injections of AAV9 vector (Mini CMV + CBA) (10^{12}) at 5-months old. (N = 20 [10 transgenic; 7 male, 3 female], [10 non-transgenic; 7 male, 3 female] for Aha1. N = 19 [9 transgenic; 6 male, 3 female], [10 non-transgenic; 6 male, 4 female] for mCherry). Each injection delivered 2 µL of AAV9 particles. At 7-months of age the mice were used for behavioral testing using the radial arm water maze (RAWM) task. Upon completion of RAWM the brains were harvested after cardiac perfusion with 0.9% saline. The right hemisphere from each mouse was dissected and hippocampus was then snap frozen and stored at -80°C until processed as previously described (128) to obtain soluble (S1) and Sarkosyl-insoluble (P3) fractions. The left hemisphere from each mouse was fixed in 4% paraformaldehyde overnight, then sucrose gradients up to 30% were used and 25 µm thick tissue sections

were generated using a sliding microtome for general histochemical staining, and 50 µm sections for stereology studies. Sections were stored at 4ºC in Dulbecco's phosphate buffered saline (PBS) supplemented with 0.065% sodium azide until they were used for immunohistochemistry.

3.3.5 Western blot and dot blot analysis

Mouse brain tissue samples were analyzed by Western blot using 4-15% SDS gradient gels (BioRad). Antibody dilutions were 1:1000 unless otherwise stated, and all secondary antibodies were used at 1:1000 (Southern Biotech). Blots were developed using ECL (Pierce) on a LAS-4000 mini imager (GE Healthcare). For dot blots, proteins were applied onto a wet nitrocellulose membrane and dried by vacuum. Dried membranes were blocked and developed as described above.

3.3.6 Semi-denaturing Western blot

Tissue was homogenized using sonication and the low-speed spin fraction was collected after centrifugation at 13,000xg for 15 min. Samples were then mixed with 2X Laemmli sample buffer (BioRad) containing 2.1% SDS, and run on a blot using 4-15% SDS gradient gels (BioRad) without boiling the samples or adding β-Mercaptoethanol (βME).

3.3.7 Radial arm water maze

The radial arm water maze (RAWM) was performed as previously described (151). Briefly, a circular black tank with a six arm metal insert was filled with water and a platform was submerged 1 cm below the surface of the water at the end of a designated

goal arm. Animals were permitted 60 seconds to locate the platform, during which time an observer blind to treatment manually scored the number of errors. An error was defined as an entry into an incorrect arm or the absence of an arm choice within 15 seconds. Mice were trained over 2 days with 12 trials per day, which were divided into 4 blocks of 3 trials each. Average errors were calculated for each mouse on day 1 and day 2. Groups were evaluated separately for each day with a one-way ANOVA using a Least Significant Difference test to compare groups.

3.3.8 Immunohistochemistry

All immunohistochemistry was done using free floating sections as previously described (152). Briefly, sections were incubated in PBS with 10% MeOH and 3% H_2O_2 to block endogenous peroxidases. After PBS washes, tissue was permeabilized for 30 minutes by 0.2% Triton X-100 with 1.83% lysine and 4% serum in PBS. Following permeabilization, tissue was incubated overnight, at room temperature with either anti-Aha1 (rat, 1:7000), or anti-T22 (rabbit, 1:700). Following PBS washes, biotinylated goat anti-rat (1:1000) or goat anti-rabbit (1:3000) secondary antibody was added for 2 hours. An ABC kit (Vectastain) was used to increase visibility. Following three PBS washes, tissue was incubated with 0.05% diaminobenzidine plus 0.5% nickel and developed with 0.03% H_2O_2. Sections were then mounted on charged slides, allowed to dry overnight and dehydrated in alcohol gradients. Slides were coverslipped with DPX following clearing with Histoclear (National Diagnostics).

Human tissue was stained as previously described using immunofluorescent secondary antibodies (131, 153). Briefly, the tissue was permeabilized as described above and

incubated at room temperature overnight with rat anti-Aha1 (1:100), and mouse anti-PHF1 (1:100). Following washes sections were incubated for 2 hours with AlexaFluor-488-labelled goat anti-rat (1:1000) or AlexaFluor 594-labelled goat anti-mouse (1:1000) secondary antibodies. Following secondary incubation, sections were stained with Neurotrace (1:25) (Invitrogen) for 20 minutes. Human tissue was also incubated in 0.1% Sudan Black B in 70% EtOH (Sigma) to reduce autofluorescence for 20 minutes and then washed three times with 0.2% Tween in PBS following fluorescent secondary. Tissue was mounted after three washes and coverslipped with ProLong Gold antifade (Invitrogen) reagent.

Sections stained for stereology were blocked and permeabilized as described above and incubated overnight at room temperature with biotinylated anti-NeuN (1:3000). Following washes, ABC conjugation, and peroxidase development, tissue was mounted on charged glass slides and allowed to dry overnight. A 0.05% cresyl violet counterstain was applied to slides then briefly and quickly destained with 0.3% acetic acid in water prior to dehydration.

3.3.9 Microscopy

Brightfield stained tissue was imaged using a Plan-Apochromat20x/0.88 objective on a Zeiss Axioscan.Z1 slide scanner. Brain tissue immunofluorescently stained was imaged using the Leica TCS SP2 for image analysis. The Zeiss LSM 880 AxioObserver laser scanning confocal microscope was used for representative images. Fields of view were selected in the cortex based on tau positive staining. A 63x/1.40PLAN APO Oil objective was used to take a minimum of 10 1 µm Z-stacked images with Argon (for tau-

positive signal in green), and Red HeNe (for Aha1-positive and Neurotrace signal in red).

3.3.10 Imaging analysis

Brightfield image analysis was performed using NearCYTE software (http://www.nearcyte.org) as previously described (131). This program was used to outline regions of interest and then thresholds were set manually until all of the user-determined positive cells were selected with as little non-specific area selected as possible. Using the batch process option, the area positive ratio was automatically calculated for each slide.

Fluorescent image analysis was performed using ImageJ. Background was subtracted from the red channel using the Gaussian Blur tool (Radius = 50um) and then the new blurred image was subtracted from the original image. The red channel was also despeckled before image analysis. Both channels were set to a consistent threshold and then colocalization between the red and green channels were quantified with a Pearson's coefficient. The intensity of red fluorescence was also measured in order to make a scatter plot showing levels of Aha1 in relation to Braak staging.

3.3.11 Stereology

Neurons were stained with anti-NeuN and cresyl violet, and those positive for both were counted in the CA1 of the hippocampus. A computerized stereological system, connected to a Leica DM4000B microscope with a Prior motorized stage, was used to outline the area using distinct landmarks in the brain at 4x magnification (153, 154). Every 8th section was sliced at 50um to be used for stereology, and only sections

containing hippocampi (as determined by analyzer) were counted (mCherry N = 7 animals, ~9 sections/animal, ~5 reference points/section; Aha1 N= 8, ~9 sections/animal, ~5 reference points/section). After the initial analysis, the mCherry control group was reanalyzed at a higher stringency level. Neurons were counted in this region by using randomly designated areas in the computer generated grid using a 100x oil immersion lens. Neurons were counted when they were located within the three-dimensional dissectors or touching the inclusion lines, and the top and bottom 1 µm of tissue were excluded. After analysis of all tissue, the number of neurons/animal were multiplied by 4.5 in order to reflect the total number of neurons throughout the hippocampus.

3.3.12 Statistical analysis

To compare two groups, a t-test was used. Groups larger than two were evaluated using a one-way ANOVA with Dunnett's multiple comparison test. P values below 0.05 were considered significant.

3.3.13 Study approval

All studies were carried out following the guidelines set by the University of South Florida's Institutional Animal Care and Use Committee (IACUC) in accordance with the Association for Assessment and Accreditation of Laboratory Animal Care International (AALAC) regulations. All human tissue was acquired under approved Institutional Review Board (IRB) protocols for the University of California, Irvine. Patient samples were deidentified and approved for studies of this nature with written informed consent to use the tissue for research purposes.

3.4 Results

3.4.1 Aha1 co-localization with tau tangles correlates with disease progression in human AD brain.

Our previous work has shown that Aha1 overexpression led to increased insoluble tau in cell models. However, the relevance of this finding *in vivo* and more importantly, in a clinical population, was not clear. Therefore, we evaluated post-mortem human brain samples from patients with AD or healthy age-matched controls for Aha1 localization in relation to tau tangles (Fig. 3.1A). We found a significant increase in the amount of co-localization between Aha1 and tau tangles as shown by immunofluorescence (pS396/404, PHF1) in AD samples compared to control (Fig. 3.1B). Additionally, there was a positive correlation between Aha1 immunofluorescence intensity and tau Braak staging (Fig. 3.1C). This suggests Aha1 is involved in pathological tau progression providing clinical significance for Aha1 in tauopathies such as AD. These findings provide a clear rationale for investigating the link between Aha1 and tau pathology.

3.4.2 Aha1 overexpression in rTg4510 mice increased insoluble tau species.

In order to investigate the role of Aha1 *in vivo*, five-month old rTg4510 mice received bilateral hippocampal injections of AAV9-Aha1 (n = 9) or AAV9-mCherry (n = 8) (Fig. 3.2A). Immunohistochemical staining revealed that Aha1 was overexpressed throughout the hippocampus, suggesting a robust effect of the virus (Fig. 3.2B). After confirming viral expression throughout the hippocampus, the right hippocampi was used for biochemical analysis of several tau species, including Sarkosyl-insoluble tau. Aha1 overexpression significantly increased total monomeric and multimeric Sarkosyl-insoluble

tau in the hippocampus (Fig. 3.3A and B). Two different phosphorylated tau species (pS396/404 and pT231) were also examined, however, no significant differences were detected suggesting that Aha1 overexpression does not affect these specific phosphorylated tau species (Fig. 3.3C and D). Additionally, Sarkosyl-insoluble tau was not detected in wild-type mice, however there was a modest increase in soluble tau species in wild-type mice overexpressing Aha1, suggesting that Aha1 could interact with soluble, wild-type tau (Fig. 3.4A).

3.4.3 In vivo, Aha1 overexpression increases toxic tau oligomers

In addition to the increased insoluble tau, Aha1 overexpression also increased toxic T22-tau oligomer levels (131). Low-speed spin lysate taken from both individual mouse samples (Fig. 3.5A and B) as well as in pooled samples from each treatment group were run on a dot blot to check T22-tau oligomer levels (Fig. 3.5C and D). Both the individual samples, as well as the pooled samples show an increase in oligomeric tau. This increase of T22-tau oligomers in Aha1 overexpressing mice was further confirmed using immunohistochemistry, where free floating sections from the left hippocampi were stained with T22 antibody (Fig. 3.5E and F). Additionally, a semi-denaturing Western blot was run and again we show that Aha1 overexpressing mice have significantly increased T22-tau oligomers (Fig. 3.5G and H).

3.4.4 Aha1 overexpression in rTg4510 mice leads to neuronal loss and cognitive impairments.

Using unbiased stereology, rTg4510 mice overexpressing Aha1 showed a significant reduction in hippocampal CA1 neurons compared to mCherry controls (Fig.

3.6A and B). This suggests that Aha1 overexpression enhances neuronal loss in the rTg4510 mice. Learning and memory were evaluated in AAV9-Aha1 (n=9) and AAV9-mCherry (n=8) injected mice using the two-day radial arm water maze (RAWM). The RAWM is a spatial learning and memory task that evaluates both working and reference memory (151, 155). Animals overexpressing Aha1 made significantly more errors in locating the submerged escape platform compared to mCherry overexpressing littermates, demonstrating a memory recall deficit (Fig. 3.6C). This suggests that the enhanced neurotoxicity seen in the mice overexpressing Aha1 is significant enough to affect learning and memory as well. Overall, these data demonstrate that Aha1 enhances Hsp90-mediated tau aggregation and this interaction results in increased oligomeric and insoluble tau concomitant with neuronal loss and memory deficits.

3.5 Discussion

Here, we have demonstrated that overexpression of the co-chaperone Aha1 leads to a significant increase of pathological tau in the rTg4510 mouse model. We also identified the clinical relevance of Aha1, identifying that there is an increase in Aha1 levels and Aha1 is more highly co-localized with tau tangles in AD brain tissue. Taken together, this work demonstrates the importance of focusing on Aha1 as a therapeutic target for tauopathies.

Our previous work has focused on the impact of Aha1 overexpression on tau pathology *in vitro* so it was important to demonstrate that this finding would translate *in vivo* as well. Several other Hsp90 co-chaperones have also been shown to affect tau

pathology. For instance, FKBP51 has also been shown to increase oligomeric tau in the rTg4510 mouse model (131). Another immunophilin, FKBP52, was shown to bind directly to P301L tau and induce oligomer formation (156). Additionally, overexpression of the co-chaperone Cdc37 has been shown to preserve phosphorylated tau *in vitro* (157). There is also one co-chaperone that has been shown to promote the degradation of tau *in vivo*. The immunophilin, CyP40, has been shown to reduce the amount of oligomeric tau and preserve neurons in rTg4510 mice (49). While there are many co-chaperones that can affect tau pathology, both negatively and positively, Aha1 is a unique therapeutic target because of how it affects Hsp90. As mentioned in previous chapters, Aha1 is the only known stimulator of the ATPase activity of Hsp90. This means that using an inhibitor to target Aha1 may have a similar effect to using an Hsp90 inhibitor.

This work has shown that Aha1 overexpression led to an increase in both oligomeric and insoluble tau levels *in vivo*, and this increase in pathological tau manifested in cognitive deficits and neuronal loss. With this information, future studies could investigate the potential therapeutic effects of Aha1 inhibition on tau pathology *in vivo*.

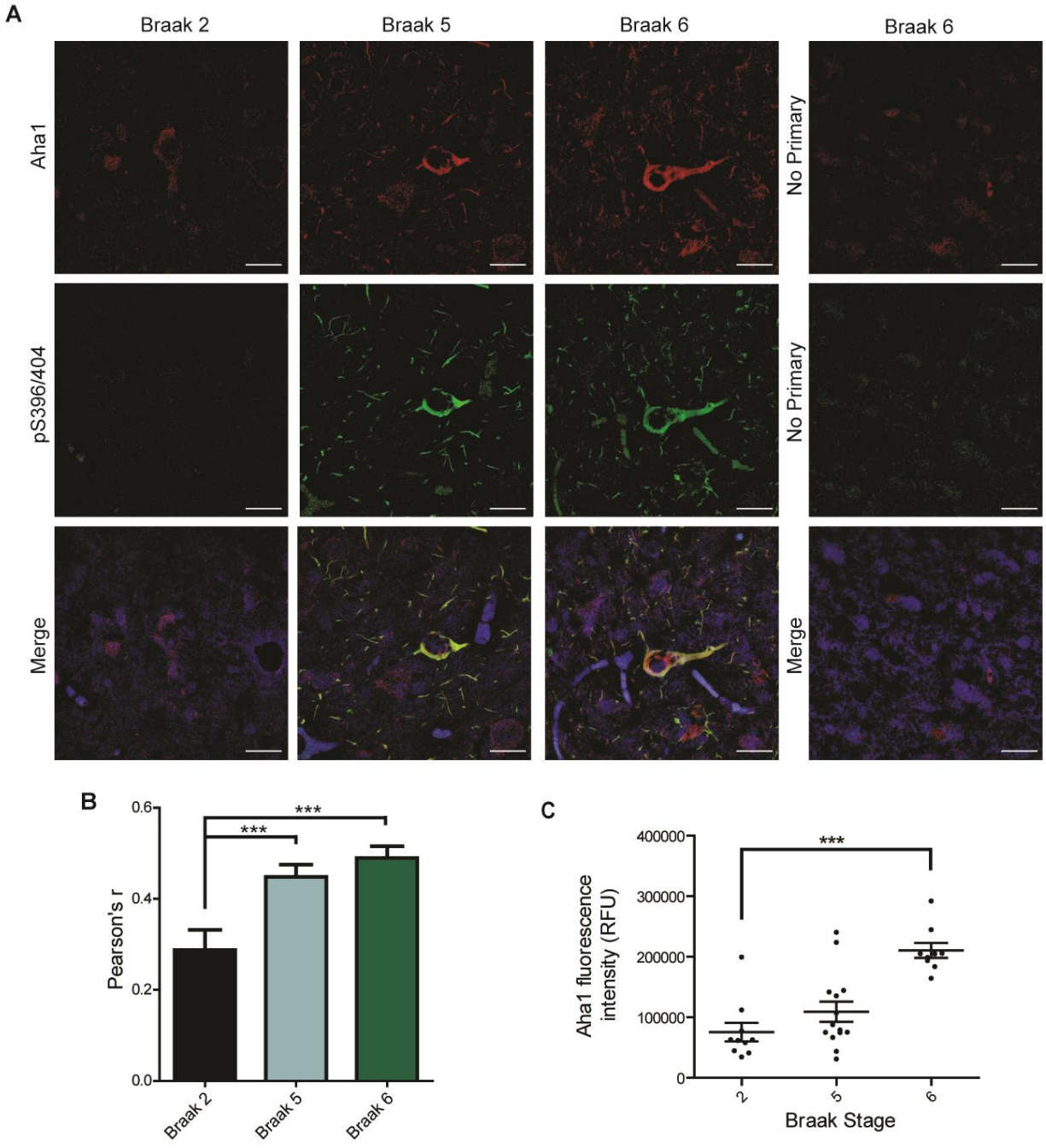

Figure 3.1. Human AD samples show co-localization between Aha1 and tau tangles. (A) Tissue samples from the medial temporal gyrus of patients at Braak stage 2, 5 or 6 were stained for Aha1 (Red), pS396/404 tau tangles (Green) and neuronal nissl (Neurotrace, Blue) and imaged using confocal microscopy, images taken at 60x.

Scale bar represents 20 µm. Representative no primary sections from a Braak stage 6 sample are shown. . (B) Quantification of co-localization between Aha1 and phosphorylated tau tangles (pS396/404) (Results represent the mean Pearson's correlation coefficient ± SEM, n=10 images; *** = $p<0.001$). (C) Scatter plot of the intensity of Aha1 fluorescence and Braak staging (Results represent the mean fluorescence intensity ± SEM; Braak stage 2: n=10 images, Braak stage 5: n=14 images, Braak stage 6: n=9 images; *** = $p<0.001$).

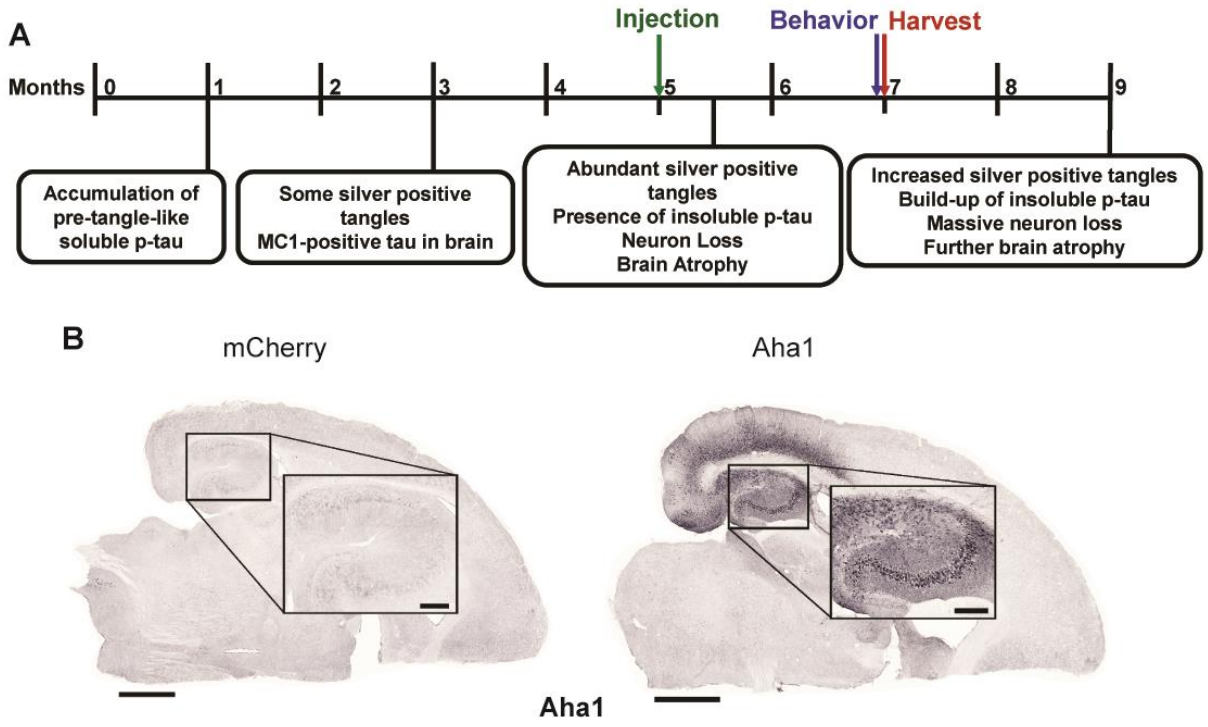

Figure 3.2. Viral transduction leads to sustained overexpression of Aha1 in the hippocampus of rTg4510 mice. (A) Characteristic phenotype of rTg4510 tau transgenic mouse model along with experimental design time points. (B) Representative images of brain sections showing viral expression of Aha1 protein in AAV9 injected Aha1 and mCherry control littermates. Scale bars represent 1000 µm for the whole slice and 250 µm for the inset.

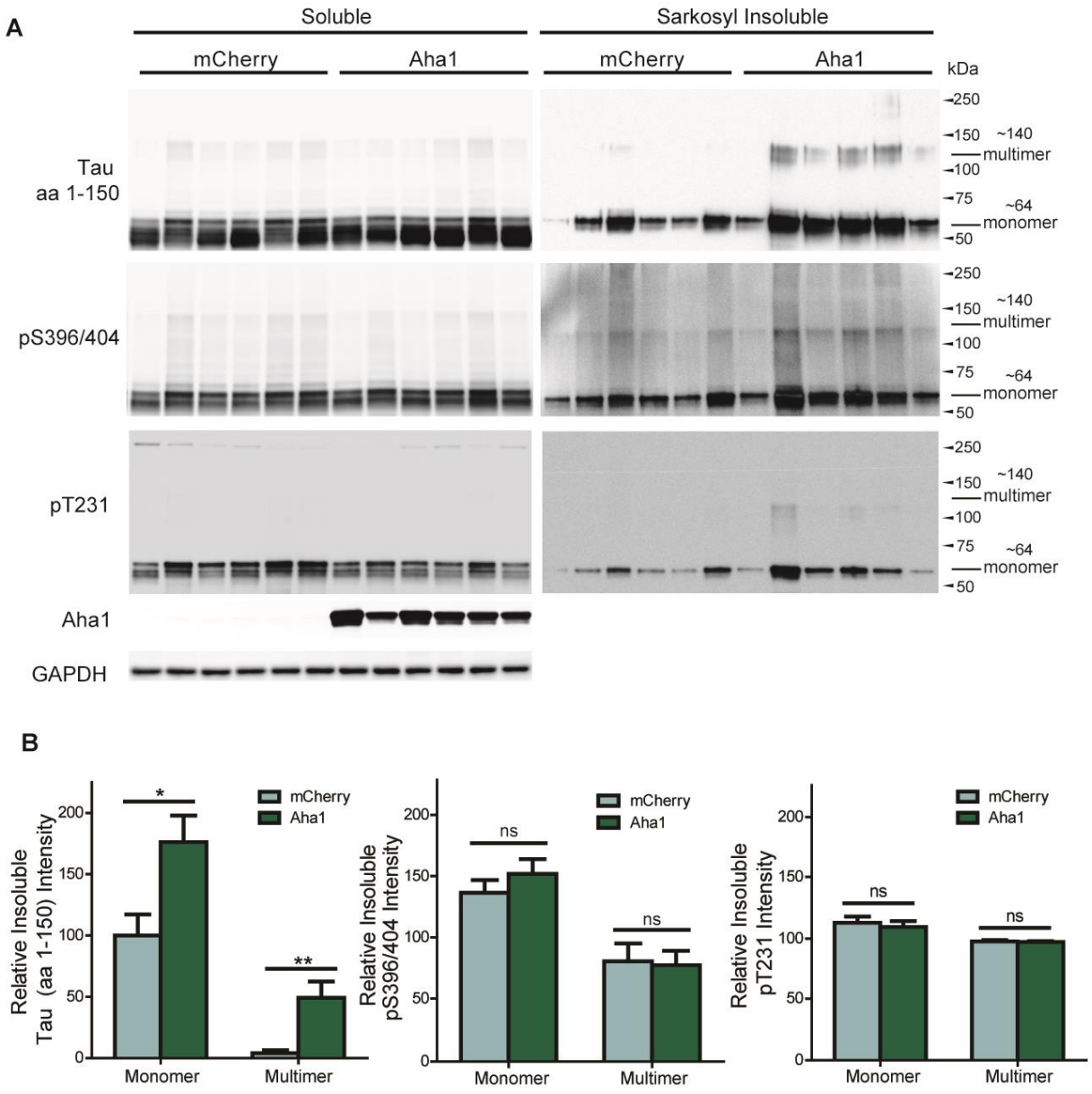

Figure 3.3. Aha1 overexpression in rTg4510 mice leads to increases in insoluble tau species. (A) Western blot analysis of soluble and Sarkosyl-insoluble fractions from hippocampal tissue of rTg4510 mice expressing either AAV9-Aha1 or AAV9-mCherry. Six representative samples from AAV9-Aha1 and AAV9-mCherry injected mice are shown. (B) Quantification of Western blots of Sarkosyl-insoluble total (aa 1-150),

pS396/404 and pT231 tau (Results represent the mean ± SEM relative to the level of monomeric tau in AAV9-mCherry injected mice; mCherry, n=8; Aha1, n=9; * = $p < 0.05$, ** = $p<0.01$).

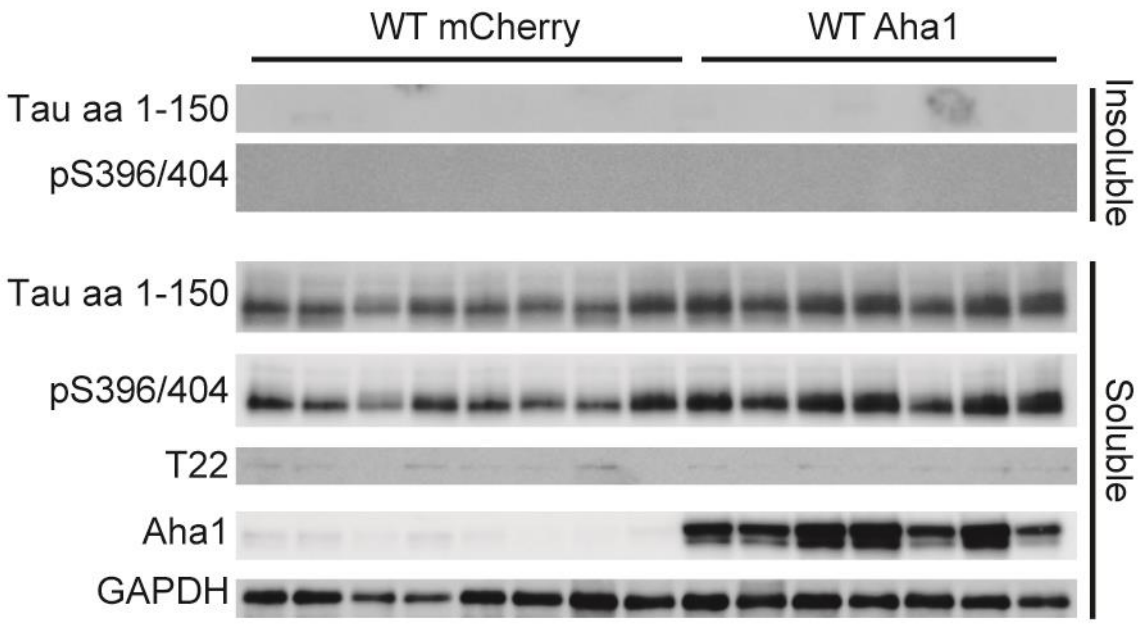

Figure 3.4. **Tau solubility in wild-type mice**. (A) Western blot analysis of soluble and Sarkosyl-insoluble fractions from hippocampal tissue of wild-type mice expressing either AAV9-Aha1 (n=7) or AAV9-mCherry (n=8). One rTg4510 mouse sample was included as a comparison.

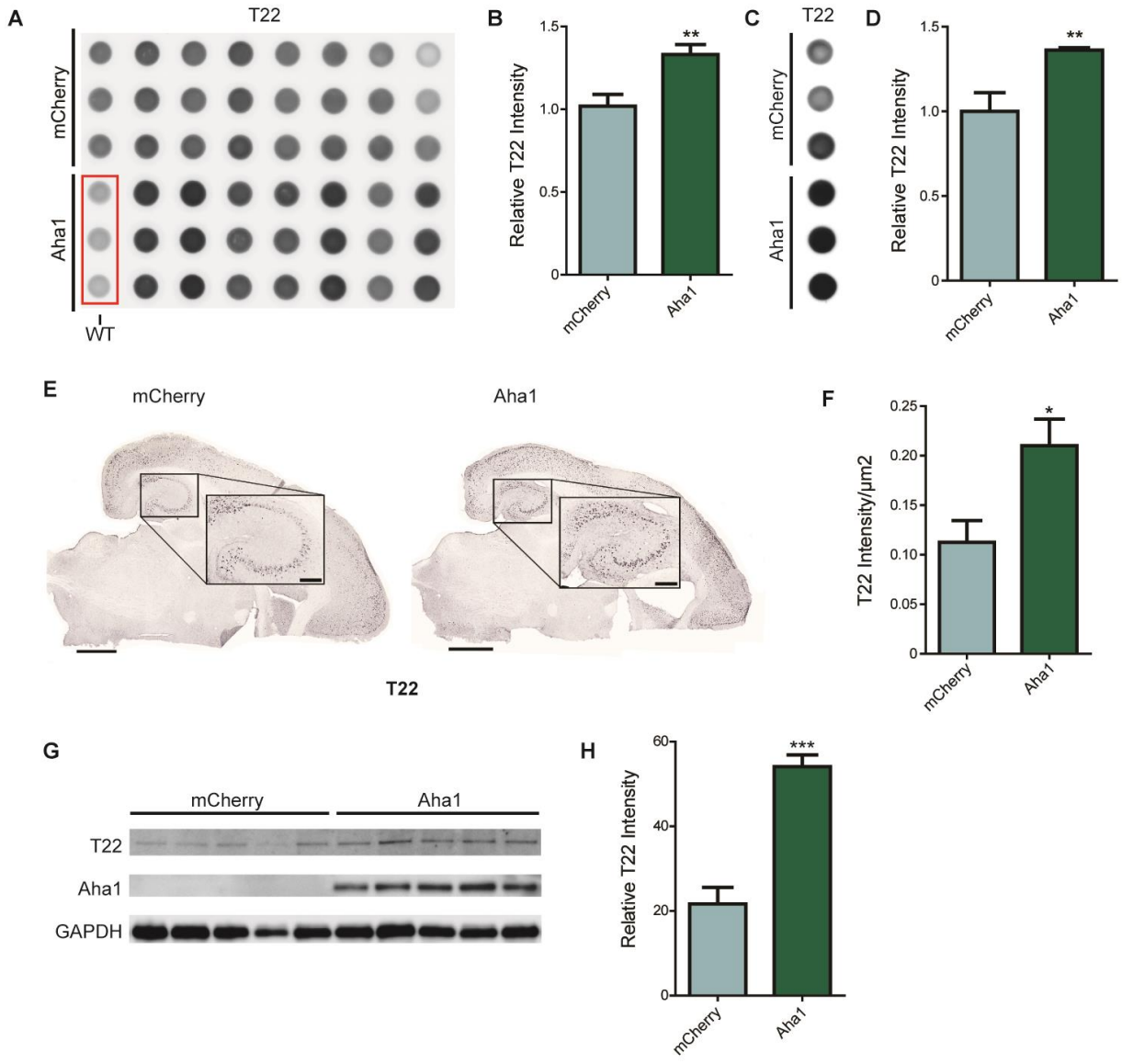

Figure 3.5. Aha1 overexpression in rTg4510 mice leads to increases in pathological tau species. (A) Dot blot of hippocampal tissue of individual mice shown in triplicate probed by T22. (B) Quantification of dot blot (Results represent the mean ± SEM; mCherry, n=8; Aha1, n=8; **p < 0.01). (C) Dot blot of pooled hippocampal tissue shown in triplicate probed by T22. (D) Quantification of dot blot (Results represent the mean ± SEM of triplicate samples taken from the pooled fractions; n=3; * = p < 0.05).

(E) Representative images of brain tissue slices stained with T22 from AAV9-mCherry and AAV9-Aha1 injected mice. Scale bars represent 1000 µm for the whole slice and 250 µm for the inset. (F) Quantification of the T22 positive area in the hippocampal field of view (inset from E) (Results represent the mean ± SEM; mCherry, n=8; Aha1, n=9; *$p < 0.05$). (G) Samples from AAV9-Aha1 and AAV9-mCherry mice were run on a semi-denaturing gel and probed by T22 (1:500) along with other antibodies as indicated. (H) Quantification of T22 Western blot (~75 kDa, results represent the mean ± SEM; mCherry, n=6; Aha1, n=7).

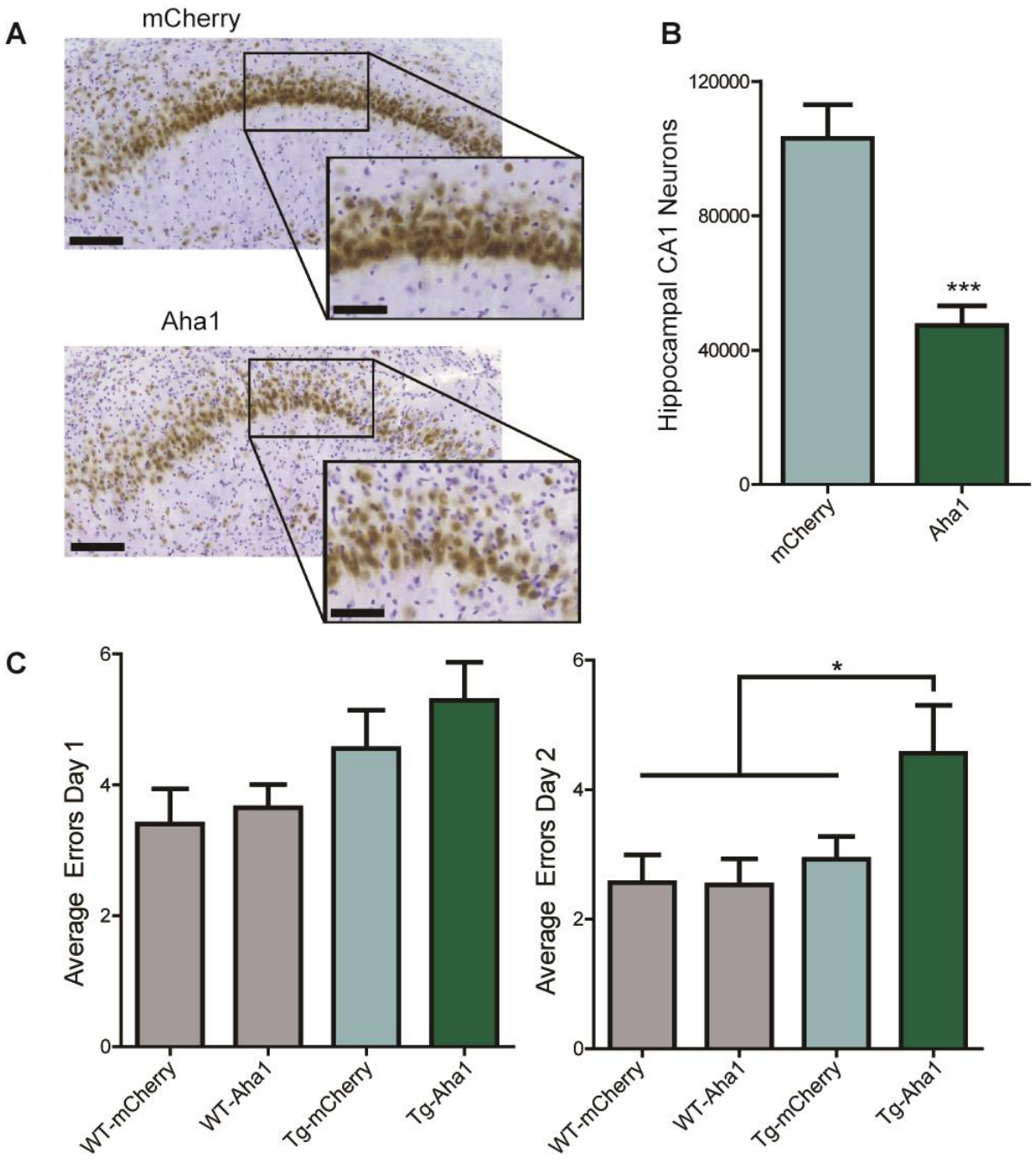

Figure 3.6. Aha1 overexpression in rTg4510 mice leads to cognitive impairments. (A) Representative images of NeuN stained neurons in the CA1 region of the hippocampus (brown) counter stained with cresyl violet (purple) from AAV9-mCherry and AAV9-Aha1 injected mice. Inset scale bars represent 100 µm. (B) Quantification of

unbiased stereology (Results represent the mean ± SEM; mCherry, n=7; Aha1, n=8; $p = 0.0003$). (C) Radial arm water maze (RAWM) was performed on AAV9-Aha1 and AAV9-mCherry rTg4510 (Tg) and wild-type (WT) littermates as indicated. Average errors from Day 1 (training) and Day 2 (memory) are shown. (Results represent the mean ± SEM; $n \geq 9$; * = $p < 0.05$).

Chapter Four:

Aha1 knock-down results in reduced tau pathology and neuroprotection in rTg4510 mice

4.1 Abstract

The Hsp90 chaperone network has been studied for its role in tauopathies for some time. Many Hsp90/co-chaperone complexes have been implicated for their role, both positive and negative, in tau pathology. For example, the FKBP51/Hsp90 complex can worsen tau pathology, while the CyP40/Hsp90 complex is able to disaggregate tau fibrils and rescue neurotoxicity *in vivo*. Recently, the co-chaperone Aha1, in complex with Hsp90, was shown to worsen tau pathology in rTg4510 mice providing another co-chaperone complex to potentially target. In this study, we have shown that pathological tau levels are reduced when Aha1 is knocked-down in the rTg4510 mouse model. Additionally, Aha1 knock-down preserves neuronal loss in the CA1 of the hippocampus. Our data support the role of the Aha1/Hsp90 complex in tau pathology and provide additional support of this complex as a target to treat tauopathies.

4.2 Introduction

Current therapeutics for the treatment of tauopathies are very limited and focus only on the symptoms of the disease (158). Disease-modifying treatments for tauopathies are sorely needed but so far these treatments have failed in clinical trials

(159). Hsp90 inhibitors were thought to be a possible candidate for treating tauopathies but have shown toxicities in clinical populations (17). Since then, some researchers have switched to focus on targeting Hsp90 co-chaperones instead, with the hope of more specificity and less toxicity. Previous work focusing on co-chaperones of Hsp90 have also shown promise in reducing toxic tau species but so far none have been successful in transitioning to the clinic (101–104). The co-chaperone Aha1 is a relatively novel co-chaperone in the field of tauopathies and because of its stimulatory function on the ATPase activity of Hsp90, Aha1 offers a unique therapeutic target (41).

While Aha1 is a novel target in the field of tauopathies, it has been studied for its role in both cancer and cystic fibrosis in the past. Inhibition of Aha1 has been found to be beneficial in both cancer and cystic fibrosis and previous work from our lab found that overexpression of Aha1 is detrimental in tauopathy (38, 41, 126). Therefore, developing a therapeutic that targets Aha1 could be advantageous in multiple diseases. Previous work has used both genetic inhibition, as well as novel Aha1 inhibitors. One group has shown that gene silencing of Aha1 via siRNA led to a rescue of misfolded CFTR in cystic fibrosis (126). Other work has focused on screening novel compounds to be used as Aha1 inhibitors in the treatment of both cancer and cystic fibrosis (143, 160).

Here we sought to knock-down Aha1 *in vivo* using shRNA packaged inside adeno-associated virus serotype 9 (AAV9). We found that Aha1 was knocked-down in the rTg4510 mice, and the reduced levels of Aha1 resulted in decreased, pathologically relevant tau species. Additionally, Aha1 knock-down resulted in a preservation of neurons in the CA1 of the hippocampus. Our findings suggest that knock-down of Aha1

is a potential target for the treatment of tauopathies because of the reductions in pathological tau accumulation as well as the neuroprotective effects seen.

4.3 Materials and methods

4.3.1 Materials

Antibodies: Anti-Aha1 (StressMarq, SMC-172D), anti-GAPDH (Proteintech, 60004-1-Ig), anti-NeuN (Millipore, MAB377B), H-150 anti-tau (Santa Cruz Biotechnology, sc-5587), anti-total human tau (Dako, A0024). PHF1 anti-tau (pS396/404) was a kind gift from Dr. Peter Davies. T22 anti-tau oligomer was a kind gift from Dr. Rakez Kayed.

Plasmids: The shRNA-Aha1 and shRNA-scrambled plasmids were ordered from Sigma.

4.3.2 Cell culture and transfection

N2A cells were cultured in MEM media supplemented with 10% FBS and 1% Penicillin-Streptomycin (Invitrogen). Transfections were performed with 2.5 µL Lipofectamine 2000 (Invitrogen) per 1 µg of DNA, which was incubated in serum-free Opti-MEM for 5 minutes before adding the mixture dropwise to the cells. Cells were harvested in RIPA buffer (10 mM Tris-Cl, 1 mM EDTA, 1% Triton X-100, 0.1% sodium deoxycholate, 0.1% SDS, 140 mM NaCl, pH 7.4) containing protease inhibitors.

4.3.3 Viral vector production

Adeno-associated virus (AAV) serotype 9-shRNA-Aha1 and AAV9-shRNA-scrambled were generated in our lab for murine gene therapy studies. The shRNA-Aha1 (CCGGCAACAGGAAAGGCAAACTTATCTCGAGATAAGTTTGCCTTTCCTGTTGTTTT

TG) and shRNA-scrambled were placed in a pTR12.1 backbone with a U6 promoter, followed by a chicken-β-actin (CBA) promoter and mCherry to observe viral expression.

4.3.4 Western blot and dot blot analysis

Cell and mouse brain samples were analyzed by Western blot using 4-15% SDS gradient gels (BioRad). Antibody dilutions were 1:1000 unless otherwise stated and all secondary antibodies were used at 1:1000 (Southern Biotech). Blots were developed using ECL (Pierce) on a LAS-4000 mini imager (GE Healthcare). For dot blots, proteins were applied onto a wet nitrocellulose membrane and dried by vacuum. Dried membranes were blocked and developed as described above.

4.3.5 Immunohistochemistry

All immunohistochemistry was done using free floating sections as previously described (152). Briefly, sections were incubated in PBS with 10% MeOH and 3% H_2O_2 to block endogenous peroxidases. After PBS washes, tissue was permeabilized for 30 minutes by 0.2% Triton X-100 with 1.83% lysine and 4% serum in PBS. Following permeabilization, tissue was incubated overnight, at room temperature with either anti-PHF1 (mouse, 1:5000), or anti-total human tau (rabbit, 1:100000). Following PBS washes, biotinylated goat anti-mouse (1:3000) or goat anti-rabbit (1:3000) secondary antibody was added for 2 hours. An ABC kit (Vectastain) was used to increase visibility. Following three PBS washes, tissue was incubated with 0.05% diaminobenzidine plus 0.5% nickel and developed with 0.03% H_2O_2. Sections were then mounted on charged slides, allowed to dry overnight and dehydrated in alcohol gradients. Slides were coverslipped with DPX following clearing with Histoclear (National Diagnostics). Gallyas

silver stain was performed as previously described for non-paraffin imbedded tissue (148).

Mouse tissue was also stained immunofluorescently as previously described (131, 153). Briefly, the tissue was permeabilized as described above and incubated at room temperature overnight with rat anti-Aha1 (1:100). Following washes sections were incubated for 2 hours with AlexaFluor-647-labelled goat anti-rat (1:1000) secondary antibody. Tissue was then mounted after three washes and coverslipped with ProLong Gold antifade (Invitrogen) reagent.

Sections stained for stereology were blocked and permeabilized as described above and incubated overnight at room temperature with biotinylated anti-NeuN (1:3000). Following washes, ABC conjugation, and peroxidase development, tissue was mounted on charged glass slides and allowed to dry overnight. A 0.05% cresyl violet counterstain was applied to slides then briefly and quickly destained with 0.3% acetic acid in water prior to dehydration.

4.3.6 Microscopy

Both brightfield and fluorescently stained tissue was imaged using a Plan-Apochromat20x/0.88 objective on a Zeiss Axioscan.Z1 slide scanner.

4.3.7 Imaging analysis

Brightfield and fluorescent image analysis was performed using NearCYTE software (http://www.nearcyte.org) as previously described (131). This program was used to outline regions of interest and then thresholds were set manually until all of the user-determined positive cells were selected with as little non-specific area selected as

possible. Using the batch process option, the area positive ratio was automatically calculated for each slide.

4.3.8 Stereology

Neurons were stained with anti-NeuN and cresyl violet, and those positive for both were counted in the CA1 of the hippocampus. A computerized stereological system, connected to a Leica DM4000B microscope with a Prior motorized stage, was used to outline the area using distinct landmarks in the brain at 4x magnification (153, 154). Every 8^{th} section was sliced at 50um to be used for stereology, and only sections containing hippocampi (as determined by analyzer) were counted. Neurons were counted in this region by using randomly designated areas in the computer generated grid using a 100x oil immersion lens. Neurons were counted when they were located within the three-dimensional dissectors or touching the inclusion lines, and the top and bottom 1 µm of tissue were excluded. After analysis of all tissue, the number of neurons/animal were multiplied by 4.5 in order to reflect the total number of neurons throughout the hippocampus.

4.3.9 Statistical analysis

To compare two groups, a t-test was used. Groups larger than two were evaluated using a one-way ANOVA with Dunnett's multiple comparison test. P values below 0.05 were considered significant.

4.3.10 Study approval

All studies were carried out following the guidelines set by the University of South Florida's Institutional Animal Care and Use Committee (IACUC) in accordance with the Association for Assessment and Accreditation of Laboratory Animal Care International (AALAC) regulations.

4.4 Results

4.4.1 Developing an shRNA-Aha1 AAV9 virus

Several mouse shRNA-Aha1 plasmids were tested for knock-down efficiency in N2A cells because of the high levels of endogenous Aha1 (Fig. 4.1A). All three shRNA plasmids were able to reduce the levels of Aha1 compared to control, however shAha1-3 led to the greatest reductions so we chose to move forward with that plasmid (Fig. 4.1B). From there, both the shRNA-Aha1 and shRNA scramble, as our control virus, were inserted into an AAV9 viral vector along with mCherry on a separate promoter to verify viral expression (Fig. 4.1C).

4.4.2 Knock-down of Aha1 is confirmed after three months of expression

Five-month-old rTg4510 mice received bilateral hippocampal injections of AAV9-shRNA-Aha1 (shAha1, n=8) or AAV9-shRNA-scrambled (scrambled, n=10), with three months of viral expression. Aha1 knock-down was confirmed both with Western blot (Fig. 4.2A and B) as well as with immunofluorescence (Fig. 4.2C and D), showing that both the left and right hippocampi had a significant reduction in Aha1 levels.

4.4.3 Aha1 knock-down in rTg4510 mice decreased pathological tau species and reduced neurotoxicity.

Our previous work has shown that knock-down of Aha1 prevents insoluble tau accumulation *in vitro* so we chose to stain for Gallyas-silver positive tangles, which are a traditional pathological hallmark of AD and other tauopathies (41). The rTg4510 mice are a good model to use because they are one of the only transgenic models that produce Gallyas-silver positive tangles. We found that in our shAha1 mice, there was a significant reduction in the amount of Gallyas-silver positive tangles (Fig. 4.3A and B). After seeing a reduction in pathologically relevant tau species, we wanted to look at whether Aha1 knock-down affected neurotoxicity. Using unbiased stereology, neurons from the CA1 of the hippocampus were counted. Aha1 knock-down led to a complete rescue of hippocampal CA1 neurons (Fig 4.4A and B).

4.4.4 Aha1 knock-down reduced phosphorylated but not total or oligomeric tau

We also wanted to examine other tau species to see if shAha1 has an effect on oligomeric, phosphorylated, or total tau. We found that knock-down of Aha1 led to reductions in phosphorylated tau (Fig. 4.5A-D), but did not result in reductions of total tau (Fig. 4.6A and B). We also examined oligomeric tau species via both immunohistochemistry (Fig. 4.7A and B) as well as biochemically (Fig. 4.7C and D). We did not see a significant difference in oligomeric tau species between scrambled and shAha1 mice.

4.5 Discussion

Here we show that Aha1 knock-down led to reductions in both phosphorylated and Gallyas silver positive tau tangles. In addition to less pathological tau species, we also found that Aha1 knock-down resulted in preservation of neurons in the CA1 of the hippocampus of rTg4510 mice. These findings suggest that Aha1 knock-down could potentially slow the progression of tauopathies, as the mice were injected at 5 months of age and they did not develop accumulation of pathological tau or neuronal loss at the severity that is typically seen in these mice by 8 months of age. While we did not see a difference in oligomeric tau in these mice, that could be due to a lack of robust Aha1 knock-down or it could also be a timing issue as we only examined the pathological tau accumulation at one time point. Oligomeric tau could be harder to degrade or take longer to degrade than other tau species which could explain the discrepancies seen between Aha1 overexpression and knock-down.

Previous work has also revealed the benefit of inhibiting Aha1, as this results in less Hsp90 ATPase activity, which can be beneficial especially in cancer cells. By reducing the ATPase activity of Hsp90, cancerous cells become more responsive to treatment (38). The same could be true for tauopathies as well. If the ATPase cycle of Hsp90 is slowed, it could allow more time for Hsp90 to properly deal with aggregated tau, allowing the preservation of neurons. Alternatively, Hsp90 could be holding tau in its aggregated state because it is not able to properly refold it and if Aha1 levels are reduced this could prevent Hsp90 from attempting to refold it, thereby allowing tau to be degraded by other chaperone machinery. Further examinations of the mechanism behind Aha1 mediated tau reductions are needed.

This work has demonstrated the relevance of Aha1 knock-down *in vivo*. Future studies could use Aha1 specific inhibitors *in vivo* to further progress this work. Overall, this study demonstrates that Aha1 inhibition is an important therapeutic target for treating tauopathies.

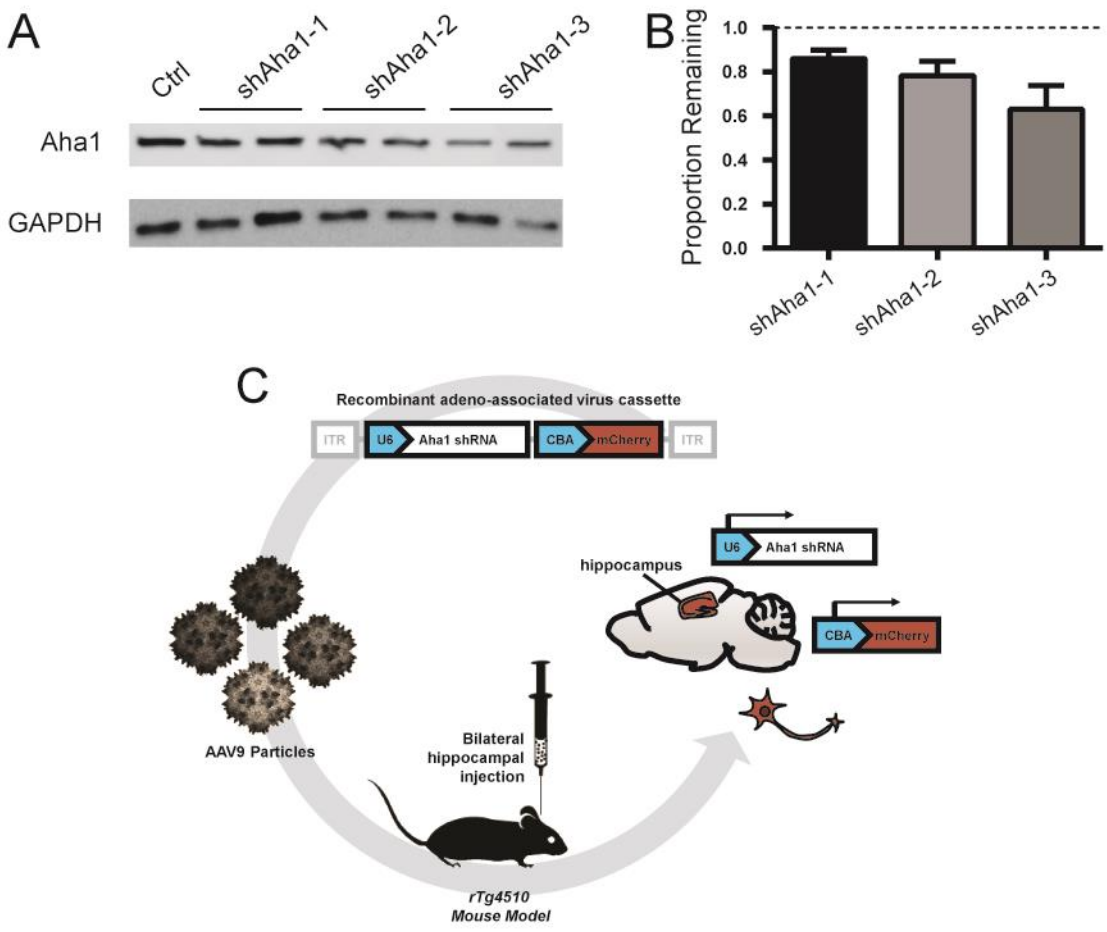

Figure 4.1. Generating shRNA-Aha1 AAV9. (A) N2A cells were transfected with shRNA-Aha1 plasmids and allowed to express for 48hr before harvesting and samples were run by Western blot. (B) Quantification of Aha1 protein reduction after treatment with shRNA. (C) Schematic of viral construct and delivery method.

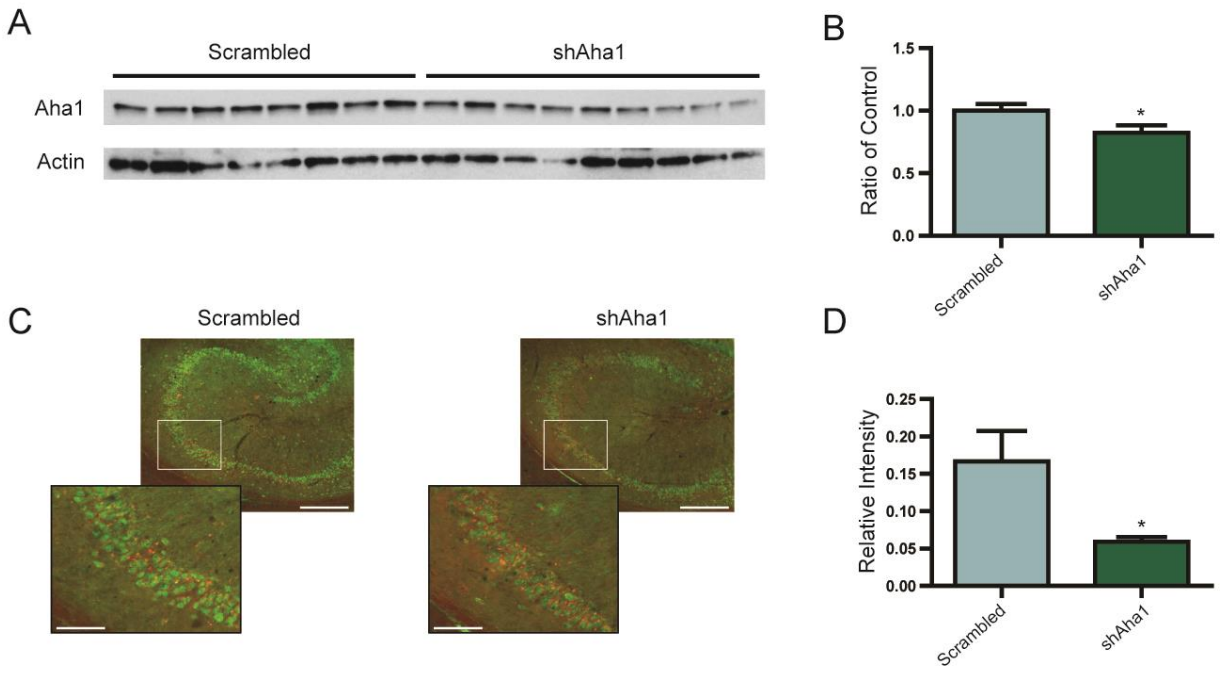

Figure 4.2. Viral transduction results in reduced Aha1 levels. (A) Samples of low-speed spin from each mouse hippocampi were analyzed by Western blot to check Aha1 knock-down. (B) Quantification of Western blot Aha1 levels relative to Actin control levels (results represent the mean ± SEM; scrambled, n=8; shAha1, n=8; *p < 0.05). (C) Representative image of Aha1 expression from AAV9-scrambled and AAV9-shAha1 mice. Scale bars represent 300 µm for the whole slice and 100 µm for the inset. (D) Quantification of the Aha1 positive area in the hippocampal field of view (results represent the mean ± SEM; scrambled, n=8; shAha1, n=6; *p < 0.05).

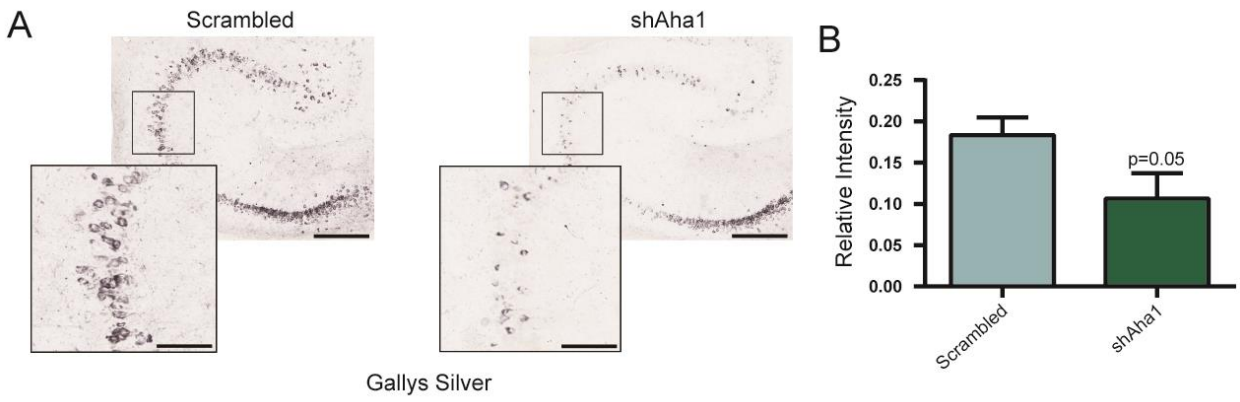

Figure 4.3. Aha1 knock-down decreases Gallyas silver positive tau tangles. (A) Representative images of brain tissue slices stained with Gallyas silver from AAV9-scrambled and AAV9-shAha1 mice. Scale bars represent 300 µm for the whole slice and 100 µm for the inset (B) Quantification of the Gallyas silver positive area in the hippocampal field of view (results represent the mean ± SEM; scrambled, n=8; shAha1, n=6; p=0.05).

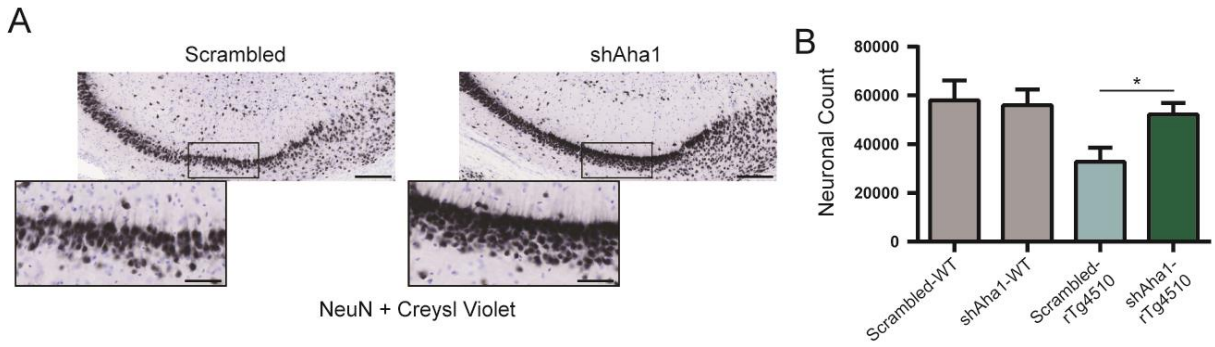

Figure 4.4. Preservation of hippocampal CA1 neurons seen with Aha1 knock-down. (A) Representative images of NeuN stained neurons in the CA1 region of the hippocampus (black) counter stained with creysl violet (purple) from AAV9-scrambled and AAV9-shAha1 mice. Scale bars represent 150 µm for the whole slice and 50 µm for the inset. (B) Quantification of unbiased stereology (results represent the mean ± SEM; scrambled-WT, n=8; shAha1-WT, n=8; scrambled-rTg4510, n=8; shAha1-rTg4510 n =6; *$p < 0.05$).

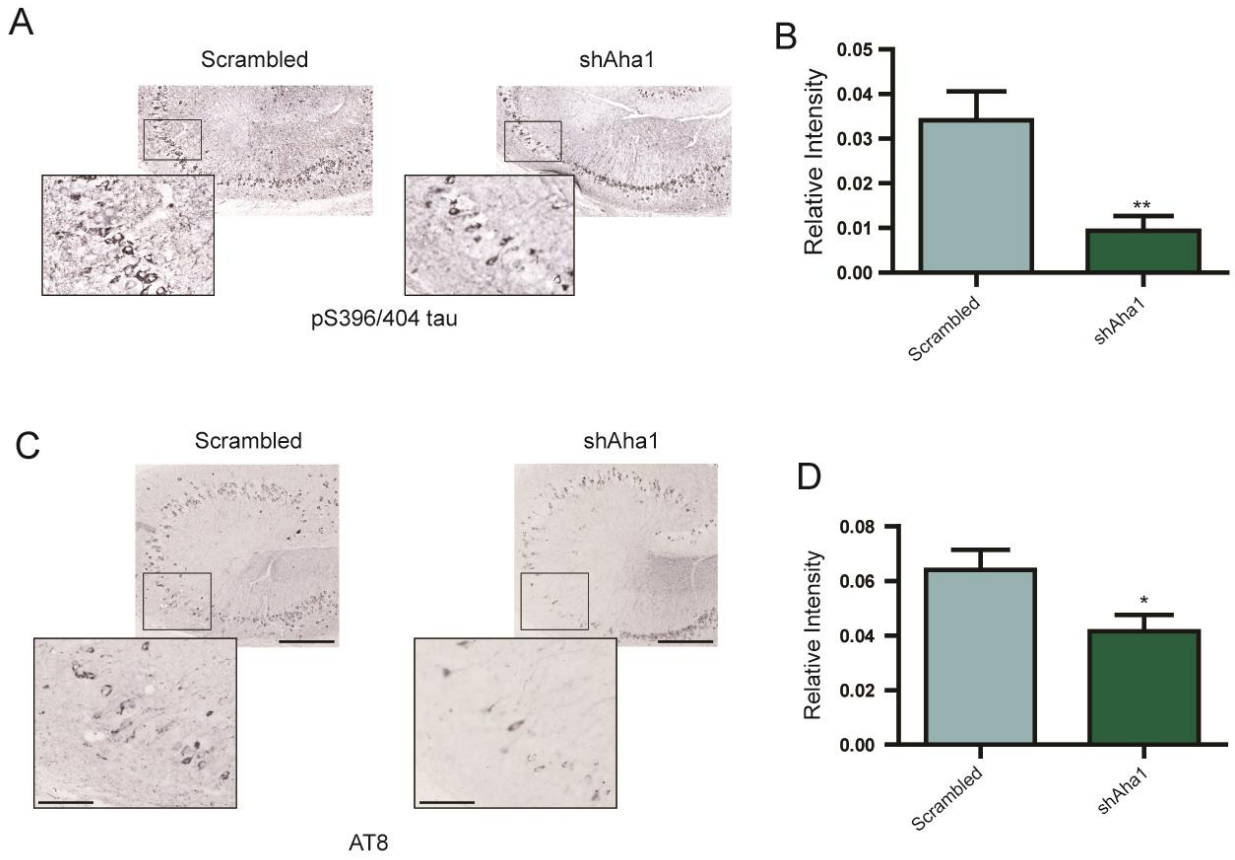

Figure 4.5. Aha1 knock-down reduces phosphorylated tau. (A) Representative images of pS396/404 stained tissue from AAV9-scrambled and AAV9-shAha1 mice. Scale bars represent 300 µm for the whole slice and 100 µm for the inset. (B) Quantification of pS396/404 positive area from hippocampal field of view (results represent the mean ± SEM; scrambled, n=8; shAha1, n=6; **p < 0.01). (C) Representative images of AT8 stained tissue from AAV9-scrambled and AAV9-shAha1 mice. Scale bars represent 300 µm for the whole slice and 100 µm for the inset. (D) Quantification of AT8 positive area from hippocampal field of view (results represent the mean ± SEM; scrambled, n=8; shAha1, n=6; **p < 0.01).

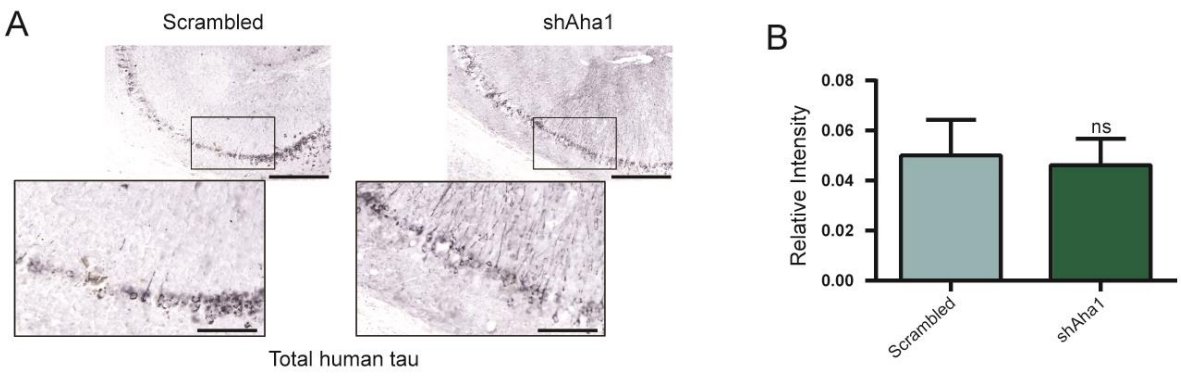

Figure 4.6. Aha1 knock-down does not lead to altered total tau levels. (A) Representative images of total human tau stained tissue from AAV9-scrambled and AAV9-shAha1 mice. Scale bars represent 300 µm for the whole slice and 100 µm for the inset. (B) Quantification of total human tau positive area from hippocampal field of view (results represent the mean ± SEM; scrambled, n=8; shAha1, n=6; ns=non-significant).

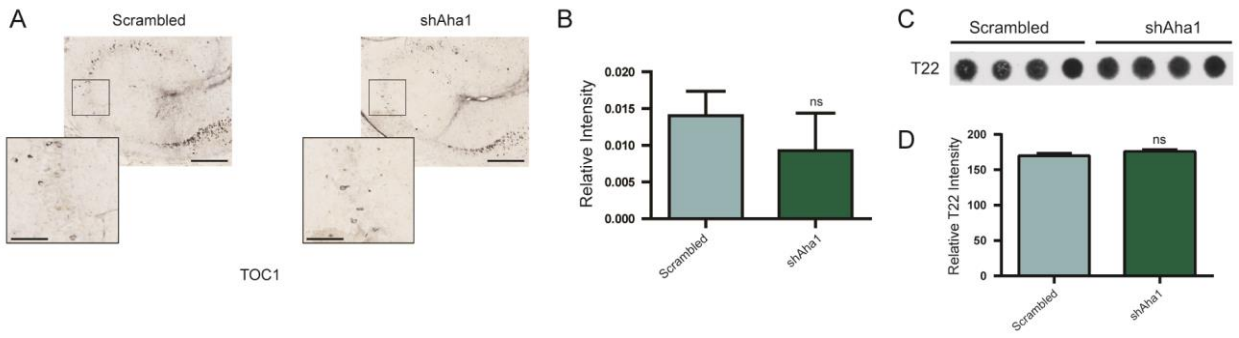

Figure 4.7. No reductions seen in oligomeric tau from Aha1 knock-down. (A) Representative images of TOC1 stained tissue from AAV9-scrambled and AAV9-shAha1 mice. Scale bars represent 300 µm for the whole slice and 100 µm for the inset. (B) Quantification of TOC1 positive area from hippocampal field of view (results represent the mean ± SEM; scrambled, n=8; shAha1, n=6; **p < 0.01). (C) Dot blot of hippocampal tissue from individual mice probed by T22. Four representative samples shown for AAV9-scrambled and AAV9-shAha1. (D) Quantification of dot blot (results represent the mean ± SEM of individual mouse samples; scrambled, n=6; shAha1, n=6; ns=non-significant).

Chapter Five:

Final considerations

This study has identified the Hsp90 co-chaperone, Aha1, as an important regulator of tau pathology. The major findings in this study demonstrate that Aha1, in complex with Hsp90, enhances tau aggregation, both in vitro and in vivo. Aha1 overexpression in rTg4510 mice leads to cognitive deficits and neuronal loss, whereas knock-down of Aha1 in the same mouse model leads to reduced pathological tau and neuronal preservation. We have shown that Aha1 is co-localized with tau tangles in the brains of human AD patients, providing a clinical link between Aha1 and tau. This study supports the need to further characterize drugs which target the Hsp90/Aha1 interaction as a therapeutic option for the treatment of AD and other tauopathies.

The Hsp90 chaperone network is highly involved in tau pathology, especially in aging and disease. The levels of many Hsp90 chaperone network family members are altered in aging and AD, suggesting that these changes may be important for aging-related diseases. Hsp90 has been the main target for modulating tau degradation, but due to toxicity and bioavailbility of Hsp90 inhibitors there has been no clinical success with Hsp90 inhibitors. Therefore, it is beneficial to try a different approach using co-chaperones, which help with specificity as well as limit the possibility of toxicity. Aha1 appears to be an excellent candidate because inhibitors of Aha1 may have a similar effect as inhibitors towards Hsp90. Additionally; Aha1/Hsp90 has a much smaller pool of potential protein interactions, which lessens the chance of toxicities.

There are some limitations with targeting Aha1 as a disease-modifying treatment for tauopathies. Currently, while there are small molecule inhibitors of Aha1, none of them have been tested for their *in vivo* effectiveness on tau pathology. Additionally, there is no pharmacokinetic, pharmacodynamics or toxicity data on these inhibitors. So while the proof-of-concept of Aha1 inhibition is reasonable, further studies into small molecule Aha1 inhibitors needs to be done. While the mechanism involving Hsp90 and tau has been well studied, further studies examining the effect of the Hsp90/Aha1 interaction on tau pathology are warranted. It seems counterintuitive that chaperone proteins would make tau pathology worse; however, that is exactly what several members of the Hsp90 chaperone network do, including FKBP51, Aha1, and several others mentioned in Chapter 1. The imbalances seen in the Hsp90 chaperone network in aging and AD shed some light on the problem, with co-chaperones like FKBP51 and Aha1 increasing with AD, while others such as CyP40 and PP5 are repressed. It seems there is a bigger picture between the Hsp90 chaperone network and tau that will need to be elucidated in order to be able to treat tauopathies.

There is also a potential link between Aha1 and tau through the tyrosine kinase c-Abl. C-Abl has been shown to modulate tau pathology and according to one study, c-Abl phosphorylation of Y223 on Aha1 promotes its interaction with Hsp90. This suggests that an upregulation of c-Abl could be a possible mechanism behind the effects of Hsp90/Aha1 on tau pathology. Further studies are needed to fully understand the link between c-Abl, Aha1 and tau.

In addition to tauopathies, Aha1 has been implicated in other diseases such as cancer and cystic fibrosis. It would be worthwhile to monitor the progress of Aha1

therapeutics in these fields as well because advancement in diseases in the periphery usually occur faster than those of the brain. We could gain useful insights into the mechanism underlying Aha1 inhibition by studying its application in other diseases.

Overall our findings suggest that the Hsp90/Aha1 complex is integral in pathological tau accumulation. Using gene silencing of Aha1 we were able to reduce pathological tau and rescue neuronal loss. This work proves that Aha1 is a worthwhile target for the treatment of tauopathies and deserves further investigation.

References

1. Reeve A, Simcox E, Turnbull D (2014) Ageing and Parkinson's disease: why is advancing age the biggest risk factor? *Ageing Res Rev* 14:19–30.

2. Terman A (2001) Garbage catastrophe theory of aging: imperfect removal of oxidative damage? *Redox Rep* 6(1):15–26.

3. Conconi M, Szweda LI, Levine RL, Stadtman ER, Friguet B (1996) Age-related decline of rat liver multicatalytic proteinase activity and protection from oxidative inactivation by heat-shock protein 90. *Arch Biochem Biophys* 331(2):232–240.

4. Rock KL, et al. (1994) Inhibitors of the proteasome block the degradation of most cell proteins and the generation of peptides presented on MHC class I molecules. *Cell* 78(5):761–771.

5. Cuervo AM, Dice JF (2000) When lysosomes get old. *Exp Gerontol* 35(2):119–131.

6. Söti C, Csermely P (2002) Chaperones and aging: role in neurodegeneration and in other civilizational diseases. *Neurochem Int* 41(6):383–389.

7. Liberek K, Lewandowska A, Zietkiewicz S (2008) Chaperones in control of protein disaggregation. *EMBO J* 27(2):328–335.

8. Miyata Y, Koren J, Kiray J, Dickey CA, Gestwicki JE (2011) Molecular chaperones and regulation of tau quality control: strategies for drug discovery in tauopathies. *Future Med Chem* 3(12):1523–1537.

9. Echeverría PC, Bernthaler A, Dupuis P, Mayer B, Picard D (2011) An interaction network predicted from public data as a discovery tool: application to the Hsp90 molecular chaperone machine. *PLoS ONE* 6(10):e26044.

10. Schopf FH, Biebl MM, Buchner J (2017) The HSP90 chaperone machinery. *Nat Rev Mol Cell Biol* 18(6):345–360.

11. Karagöz GE, et al. (2014) Hsp90-Tau Complex Reveals Molecular Basis for Specificity in Chaperone Action. *Cell* 156(5):963–974.

12. Guo T, Noble W, Hanger DP (2017) Roles of tau protein in health and disease. *Acta Neuropathol* 133(5):665–704.

13. Kovacs GG (2015) Invited review: Neuropathology of tauopathies: principles and practice. *Neuropathol Appl Neurobiol* 41(1):3–23.

14. Orr ME, Sullivan AC, Frost B (2017) A Brief Overview of Tauopathy: Causes, Consequences, and Therapeutic Strategies. *Trends Pharmacol Sci* 38(7):637–648.

15. Dickey CA, et al. (2007) The high-affinity HSP90-CHIP complex recognizes and selectively degrades phosphorylated tau client proteins. *J Clin Invest* 117(3):648–658.

16. Luo W, et al. (2007) Roles of heat-shock protein 90 in maintaining and facilitating the neurodegenerative phenotype in tauopathies. *Proc Natl Acad Sci USA* 104(22):9511–9516.

17. Bhat R, Tummalapalli SR, Rotella DP (2014) Progress in the discovery and development of heat shock protein 90 (Hsp90) inhibitors. *J Med Chem* 57(21):8718–8728.

18. Renouf DJ, et al. (2016) A phase II study of the HSP90 inhibitor AUY922 in chemotherapy refractory advanced pancreatic cancer. *Cancer Chemother Pharmacol* 78(3):541–545.

19. Thakur MK, et al. (2016) A phase II trial of ganetespib, a heat shock protein 90 Hsp90) inhibitor, in patients with docetaxel-pretreated metastatic castrate-resistant prostate cancer (CRPC)-a prostate cancer clinical trials consortium (PCCTC) study. *Invest New Drugs* 34(1):112–118.

20. Blair LJ, et al. (2013) Accelerated neurodegeneration through chaperone-mediated oligomerization of tau. *J Clin Invest* 123(10):4158–4169.

21. Brehme M, et al. (2014) A chaperome subnetwork safeguards proteostasis in aging and neurodegenerative disease. *Cell Rep* 9(3):1135–1150.

22. Kamal A, et al. (2003) A high-affinity conformation of Hsp90 confers tumour selectivity on Hsp90 inhibitors. *Nature* 425(6956):407–410.

23. Rodina A, et al. (2016) The epichaperome is an integrated chaperome network that facilitates tumour survival. *Nature* 538(7625):397–401.

24. Picard D (2002) Heat-shock protein 90, a chaperone for folding and regulation. *Cell Mol Life Sci* 59(10):1640–1648.

25. Prodromou C (2016) Mechanisms of Hsp90 regulation. *Biochem J* 473(16):2439–2452.

26. Li J, Buchner J (2013) Structure, function and regulation of the hsp90 machinery. *Biomed J* 36(3):106–117.

27. Li J, Soroka J, Buchner J (2012) The Hsp90 chaperone machinery: conformational dynamics and regulation by co-chaperones. *Biochim Biophys Acta* 1823(3):624–635.

28. Grad I, et al. (2010) The Molecular Chaperone Hsp90α Is Required for Meiotic Progression of Spermatocytes beyond Pachytene in the Mouse. *PLoS One* 5(12). doi:10.1371/journal.pone.0015770.

29. Voss AK, Thomas T, Gruss P (2000) Mice lacking HSP90beta fail to develop a placental labyrinth. *Development* 127(1):1–11.

30. Eustace BK, et al. (2004) Functional proteomic screens reveal an essential extracellular role for hsp90 alpha in cancer cell invasiveness. *Nat Cell Biol* 6(6):507–514.

31. Sreedhar AS, Kalmár E, Csermely P, Shen Y-F (2004) Hsp90 isoforms: functions, expression and clinical importance. *FEBS Lett* 562(1–3):11–15.

32. Prodromou C, et al. (2000) The ATPase cycle of Hsp90 drives a molecular "clamp" via transient dimerization of the N-terminal domains. *EMBO J* 19(16):4383–4392.

33. Panaretou B, et al. (2002) Activation of the ATPase activity of hsp90 by the stress-regulated cochaperone aha1. *Mol Cell* 10(6):1307–1318.

34. Lotz GP, Lin H, Harst A, Obermann WMJ (2003) Aha1 binds to the middle domain of Hsp90, contributes to client protein activation, and stimulates the ATPase activity of the molecular chaperone. *J Biol Chem* 278(19):17228–17235.

35. Sevier CS, Machamer CE (2001) p38: A novel protein that associates with the vesicular stomatitis virus glycoprotein. *Biochem Biophys Res Commun* 287(2):574–582.

36. Wolmarans A, Lee B, Spyracopoulos L, LaPointe P (2016) The Mechanism of Hsp90 ATPase Stimulation by Aha1. *Sci Rep* 6:33179.

37. Mollapour M, et al. (2014) Asymmetric Hsp90 N domain SUMOylation recruits Aha1 and ATP-competitive inhibitors. *Mol Cell* 53(2):317–329.

38. Dunn DM, et al. (2015) c-Abl Mediated Tyrosine Phosphorylation of Aha1 Activates Its Co-chaperone Function in Cancer Cells. *Cell Rep* 12(6):1006–1018.

39. Cancino GI, et al. (2011) c-Abl tyrosine kinase modulates tau pathology and Cdk5 phosphorylation in AD transgenic mice. *Neurobiol Aging* 32(7):1249–1261.

40. Wang X, et al. (2006) Hsp90 cochaperone Aha1 downregulation rescues misfolding of CFTR in cystic fibrosis. *Cell* 127(4):803–815.

41. Shelton LB, et al. (2017) Hsp90 activator Aha1 drives production of pathological tau aggregates. *Proc Natl Acad Sci USA* 114(36):9707–9712.

42. Harst A, Lin H, Obermann WMJ (2005) Aha1 competes with Hop, p50 and p23 for binding to the molecular chaperone Hsp90 and contributes to kinase and hormone receptor activation. *Biochem J* 387(Pt 3):789–796.

43. Hildenbrand ZL, et al. (2011) Hsp90 can accommodate the simultaneous binding of the FKBP52 and HOP proteins. *Oncotarget* 2(1–2):43–58.

44. Blundell KLIM, Pal M, Roe SM, Pearl LH, Prodromou C (2017) The structure of FKBP38 in complex with the MEEVD tetratricopeptide binding-motif of Hsp90. *PLoS ONE* 12(3):e0173543.

45. Guy NC, Garcia YA, Sivils JC, Galigniana MD, Cox MB (2015) Functions of the Hsp90-binding FKBP immunophilins. *Subcell Biochem* 78:35–68.

46. Jarczowski F, et al. (2009) FKBP36 is an inherent multifunctional glyceraldehyde-3-phosphate dehydrogenase inhibitor. *J Biol Chem* 284(2):766–773.

47. Jascur T, et al. (2005) Regulation of p21(WAF1/CIP1) stability by WISp39, a Hsp90 binding TPR protein. *Mol Cell* 17(2):237–249.

48. Mandelkow E-M, Mandelkow E (2012) Biochemistry and cell biology of tau protein in neurofibrillary degeneration. *Cold Spring Harb Perspect Med* 2(7):a006247.

49. Baker JD, et al. (2017) Human cyclophilin 40 unravels neurotoxic amyloids. *PLoS Biol* 15(6):e2001336.

50. Blackburn EA, et al. (2015) Cyclophilin40 isomerase activity is regulated by a temperature-dependent allosteric interaction with Hsp90. *Biosci Rep* 35(5). doi:10.1042/BSR20150124.

51. Giustiniani J, et al. (2015) The FK506-binding protein FKBP52 in vitro induces aggregation of truncated Tau forms with prion-like behavior. *FASEB J* 29(8):3171–3181.

52. Kamah A, et al. (2016) Isomerization and Oligomerization of Truncated and Mutated Tau Forms by FKBP52 are Independent Processes. *J Mol Biol* 428(6):1080–1090.

53. Jinwal UK, et al. (2010) The Hsp90 cochaperone, FKBP51, increases Tau stability and polymerizes microtubules. *J Neurosci* 30(2):591–599.

54. Sabbagh JJ, et al. (2014) Age-associated epigenetic upregulation of the FKBP5 gene selectively impairs stress resiliency. *PLoS ONE* 9(9):e107241.

55. Meduri G, et al. (2016) Caspase-cleaved Tau-D(421) is colocalized with the immunophilin FKBP52 in the autophagy-endolysosomal system of Alzheimer's disease neurons. *Neurobiol Aging* 46:124–137.

56. Cook C, et al. (2012) Loss of HDAC6, a novel CHIP substrate, alleviates abnormal tau accumulation. *Hum Mol Genet* 21(13):2936–2945.

57. Kekatpure VD, Dannenberg AJ, Subbaramaiah K (2009) HDAC6 modulates Hsp90 chaperone activity and regulates activation of aryl hydrocarbon receptor signaling. *J Biol Chem* 284(12):7436–7445.

58. Selenica M-L, et al. (2014) Histone deacetylase 6 inhibition improves memory and reduces total tau levels in a mouse model of tau deposition. *Alzheimers Res Ther* 6(1):12.

59. Laenger A, et al. (2009) XAP2 inhibits glucocorticoid receptor activity in mammalian cells. *FEBS Lett* 583(9):1493–1498.

60. Pinheiro S, et al. (2016) Tau Mislocation in Glucocorticoid-Triggered Hippocampal Pathology. *Mol Neurobiol* 53(7):4745–4753.

61. Silverstein AM, et al. (1997) Protein phosphatase 5 is a major component of glucocorticoid receptor.hsp90 complexes with properties of an FK506-binding immunophilin. *J Biol Chem* 272(26):16224–16230.

62. Conde R, Xavier J, McLoughlin C, Chinkers M, Ovsenek N (2005) Protein phosphatase 5 is a negative modulator of heat shock factor 1. *J Biol Chem* 280(32):28989–28996.

63. Liu F, Iqbal K, Grundke-Iqbal I, Rossie S, Gong C-X (2005) Dephosphorylation of tau by protein phosphatase 5: impairment in Alzheimer's disease. *J Biol Chem* 280(3):1790–1796.

64. Gong C-X, et al. (2004) Dephosphorylation of microtubule-associated protein tau by protein phosphatase 5. *J Neurochem* 88(2):298–310.

65. Baindur-Hudson S, Edkins AL, Blatch GL (2015) Hsp70/Hsp90 organising protein (hop): beyond interactions with chaperones and prion proteins. *Subcell Biochem* 78:69–90.

66. Jinwal UK, Koren J, Dickey CA (2013) Reconstructing the Hsp90/Tau Machine. *Curr Enzym Inhib* 9(1):41–45.

67. Ambegaokar SS, Jackson GR (2011) Functional genomic screen and network analysis reveal novel modifiers of tauopathy dissociated from tau phosphorylation. *Hum Mol Genet* 20(24):4947–4977.

68. Edkins AL (2015) CHIP: a co-chaperone for degradation by the proteasome. *Subcell Biochem* 78:219–242.

69. Dickey CA, Patterson C, Dickson D, Petrucelli L (2007) Brain CHIP: removing the culprits in neurodegenerative disease. *Trends Mol Med* 13(1):32–38.

70. Dickey CA, et al. (2008) Akt and CHIP coregulate tau degradation through coordinated interactions. *Proc Natl Acad Sci USA* 105(9):3622–3627.

71. Palubinsky AM, et al. (2015) CHIP Is an Essential Determinant of Neuronal Mitochondrial Stress Signaling. *Antioxid Redox Signal* 23(6):535–549.

72. Brychzy A, et al. (2003) Cofactor Tpr2 combines two TPR domains and a J domain to regulate the Hsp70/Hsp90 chaperone system. *EMBO J* 22(14):3613–3623.

73. Moffatt NSC, Bruinsma E, Uhl C, Obermann WMJ, Toft D (2008) Role of the cochaperone Tpr2 in Hsp90 chaperoning. *Biochemistry* 47(31):8203–8213.

74. Cox MB, Johnson JL (2011) The role of p23, Hop, immunophilins, and other co-chaperones in regulating Hsp90 function. *Methods Mol Biol* 787:45–66.

75. Calderwood SK (2015) Cdc37 as a co-chaperone to Hsp90. *Subcell Biochem* 78:103–112.

76. Jin J, et al. (2016) Mutational Analysis of Glycogen Synthase Kinase 3β Protein Kinase Together with Kinome-Wide Binding and Stability Studies Suggests Context-Dependent Recognition of Kinases by the Chaperone Heat Shock Protein 90. *Mol Cell Biol* 36(6):1007–1018.

77. Taipale M, et al. (2012) Quantitative analysis of HSP90-client interactions reveals principles of substrate recognition. *Cell* 150(5):987–1001.

78. Jinwal UK, et al. (2012) Cdc37/Hsp90 protein complex disruption triggers an autophagic clearance cascade for TDP-43 protein. *J Biol Chem* 287(29):24814–24820.

79. Sullivan W, et al. (1997) Nucleotides and two functional states of hsp90. *J Biol Chem* 272(12):8007–8012.

80. Rehn AB, Buchner J (2015) p23 and Aha1. *Subcell Biochem* 78:113–131.

81. Freeman BC, Toft DO, Morimoto RI (1996) Molecular chaperone machines: chaperone activities of the cyclophilin Cyp-40 and the steroid aporeceptor-associated protein p23. *Science* 274(5293):1718–1720.

82. Abisambra JF, et al. (2013) Tau accumulation activates the unfolded protein response by impairing endoplasmic reticulum-associated degradation. *J Neurosci* 33(22):9498–9507.

83. Rao RV, et al. (2006) Coupling endoplasmic reticulum stress to the cell-death program: a novel HSP90-independent role for the small chaperone protein p23. *Cell Death Differ* 13(3):415–425.

84. Zhang J, et al. (2013) The small co-chaperone p23 overexpressing transgenic mouse. *J Neurosci Methods* 212(2):190–194.

85. Woodford MR, et al. (2016) The FNIP co-chaperones decelerate the Hsp90 chaperone cycle and enhance drug binding. *Nat Commun* 7:12037.

86. Njemini R, Lambert M, Demanet C, Kooijman R, Mets T (2007) Basal and infection-induced levels of heat shock proteins in human aging. *Biogerontology* 8(3):353–364.

87. Lee CH, et al. (2011) Heat shock protein 90 and its cochaperone, p23, are markedly increased in the aged gerbil hippocampus. *Exp Gerontol* 46(9):768–772.

88. Berchtold NC, et al. (2008) Gene expression changes in the course of normal brain aging are sexually dimorphic. *Proc Natl Acad Sci USA* 105(40):15605–15610.

89. Loerch PM, et al. (2008) Evolution of the aging brain transcriptome and synaptic regulation. *PLoS ONE* 3(10):e3329.

90. Schülke J-P, et al. (2010) Differential impact of tetratricopeptide repeat proteins on the steroid hormone receptors. *PLoS ONE* 5(7):e11717.

91. Conconi M, Friguet B (1997) Proteasome inactivation upon aging and on oxidation-effect of HSP 90. *Mol Biol Rep* 24(1–2):45–50.

92. Cuervo AM, Dice JF (2000) Age-related decline in chaperone-mediated autophagy. *J Biol Chem* 275(40):31505–31513.

93. Mollapour M, Neckers L (2012) Post-translational modifications of Hsp90 and their contributions to chaperone regulation. *Biochim Biophys Acta* 1823(3):648–655.

94. Zhao YG, et al. (2001) Hsp90 phosphorylation is linked to its chaperoning function. Assembly of the reovirus cell attachment protein. *J Biol Chem* 276(35):32822–32827.

95. Yu X, et al. (2002) Modulation of p53, ErbB1, ErbB2, and Raf-1 expression in lung cancer cells by depsipeptide FR901228. *J Natl Cancer Inst* 94(7):504–513.

96. Blank M, Mandel M, Keisari Y, Meruelo D, Lavie G (2003) Enhanced ubiquitinylation of heat shock protein 90 as a potential mechanism for mitotic cell death in cancer cells induced with hypericin. *Cancer Res* 63(23):8241–8247.

97. Chen W-Y, et al. (2008) Tubocapsenolide A, a novel withanolide, inhibits proliferation and induces apoptosis in MDA-MB-231 cells by thiol oxidation of heat shock proteins. *J Biol Chem* 283(25):17184–17193.

98. Martínez-Ruiz A, et al. (2005) S-nitrosylation of Hsp90 promotes the inhibition of its ATPase and endothelial nitric oxide synthase regulatory activities. *Proc Natl Acad Sci USA* 102(24):8525–8530.

99. Bhat R, Tummalapalli SR, Rotella DP (2014) Progress in the discovery and development of heat shock protein 90 (Hsp90) inhibitors. *J Med Chem* 57(21):8718–8728.

100. Carman A, Kishinevsky S, Koren J, Lou W, Chiosis G (2013) Chaperone-dependent Neurodegeneration: A Molecular Perspective on Therapeutic Intervention. *J Alzheimers Dis Parkinsonism* 2013(Suppl 10). doi:10.4172/2161-0460.S10-007.

101. Pimienta G, Herbert KM, Regan L (2011) A compound that inhibits the HOP-Hsp90 complex formation and has unique killing effects in breast cancer cell lines. *Mol Pharm* 8(6):2252–2261.

102. Yu Y, et al. (2010) Withaferin A targets heat shock protein 90 in pancreatic cancer cells. *Biochem Pharmacol* 79(4):542–551.

103. Zhang T, et al. (2008) A novel Hsp90 inhibitor to disrupt Hsp90/Cdc37 complex against pancreatic cancer cells. *Mol Cancer Ther* 7(1):162–170.

104. Li T, et al. (2017) Novel Hsp90 inhibitor platycodin D disrupts Hsp90/Cdc37 complex and enhances the anticancer effect of mTOR inhibitor. *Toxicol Appl Pharmacol* 330:65–73.

105. LeMaster DM, Hernandez G (2015) Conformational Dynamics in FKBP Domains: Relevance to Molecular Signaling and Drug Design. *Curr Mol Pharmacol* 9(1):5–26.

106. Taglialatela G, Rastellini C, Cicalese L (2015) Reduced Incidence of Dementia in Solid Organ Transplant Patients Treated with Calcineurin Inhibitors. *J Alzheimers Dis* 47(2):329–333.

107. Zannas AS, Binder EB (2014) Gene-environment interactions at the FKBP5 locus: sensitive periods, mechanisms and pleiotropism. *Genes Brain Behav* 13(1):25–37.

108. De Leon JT, et al. (2011) Targeting the regulation of androgen receptor signaling by the heat shock protein 90 cochaperone FKBP52 in prostate cancer cells. *Proc Natl Acad Sci USA* 108(29):11878–11883.

109. Hall JA, Forsberg LK, Blagg BSJ (2014) Alternative approaches to Hsp90 modulation for the treatment of cancer. *Future Med Chem* 6(14):1587–1605.

110. Lee VM, Goedert M, Trojanowski JQ (2001) Neurodegenerative tauopathies. *Annu Rev Neurosci* 24:1121–1159.

111. Ballatore C, Lee VM-Y, Trojanowski JQ (2007) Tau-mediated neurodegeneration in Alzheimer's disease and related disorders. *Nat Rev Neurosci* 8(9):663–672.

112. Caughey B, Lansbury PT (2003) Protofibrils, pores, fibrils, and neurodegeneration: separating the responsible protein aggregates from the innocent bystanders. *Annu Rev Neurosci* 26:267–298.

113. Lasagna-Reeves CA, et al. (2011) Tau oligomers impair memory and induce synaptic and mitochondrial dysfunction in wild-type mice. *Mol Neurodegener* 6:39.

114. Sahara N, et al. (2007) Molecular chaperone-mediated tau protein metabolism counteracts the formation of granular tau oligomers in human brain. *J Neurosci Res* 85(14):3098–3108.

115. Blair LJ, Sabbagh JJ, Dickey CA (2014) Targeting Hsp90 and its co-chaperones to treat Alzheimer's disease. *Expert Opin Ther Targets* 18(10):1219–1232.

116. Karagöz GE, et al. (2014) Hsp90-Tau Complex Reveals Molecular Basis for Specificity in Chaperone Action. *Cell* 156(5):963–974.

117. Pratt WB, Gestwicki JE, Osawa Y, Lieberman AP (2015) Targeting Hsp90/Hsp70-based protein quality control for treatment of adult onset neurodegenerative diseases. *Annu Rev Pharmacol Toxicol* 55:353–371.

118. Neckers L, Workman P (2012) Hsp90 molecular chaperone inhibitors: are we there yet? *Clin Cancer Res* 18(1):64–76.

119. Inda C, Bolaender A, Wang T, Gandu SR, Koren J (2016) Stressing Out Hsp90 in Neurotoxic Proteinopathies. *Curr Top Med Chem* 16(25):2829–2838.

120. Butler LM, Ferraldeschi R, Armstrong HK, Centenera MM, Workman P (2015) Maximizing the Therapeutic Potential of HSP90 Inhibitors. *Mol Cancer Res* 13(11):1445–1451.

121. Hong DS, et al. (2013) Targeting the molecular chaperone heat shock protein 90 (HSP90): lessons learned and future directions. *Cancer Treat Rev* 39(4):375–387.

122. Gaali S, et al. (2015) Selective inhibitors of the FK506-binding protein 51 by induced fit. *Nat Chem Biol* 11(1):33–37.

123. Wolmarans A, Lee B, Spyracopoulos L, LaPointe P (2016) The Mechanism of Hsp90 ATPase Stimulation by Aha1. *Sci Rep* 6:33179.

124. Li J, Richter K, Reinstein J, Buchner J (2013) Integration of the accelerator Aha1 in the Hsp90 co-chaperone cycle. *Nat Struct Mol Biol* 20(3):326–331.

125. Okayama S, et al. (2014) p53 protein regulates Hsp90 ATPase activity and thereby Wnt signaling by modulating Aha1 expression. *J Biol Chem* 289(10):6513–6525.

126. Wang X, et al. (2006) Hsp90 cochaperone Aha1 downregulation rescues misfolding of CFTR in cystic fibrosis. *Cell* 127(4):803–15.

127. Ghosh S, et al. (2016) Diverging Novobiocin Anti-Cancer Activity from Neuroprotective Activity through Modification of the Amide Tail. *ACS Med Chem Lett* 7(8):813–818.

128. Ramsden M, et al. (2005) Age-dependent neurofibrillary tangle formation, neuron loss, and memory impairment in a mouse model of human tauopathy (P301L). *J Neurosci* 25(46):10637–10647.

129. Ghosh S, et al. (2015) Hsp90 C-terminal inhibitors exhibit antimigratory activity by disrupting the Hsp90α/Aha1 complex in PC3-MM2 cells. *ACS Chem Biol* 10(2):577–590.

130. Hall JA, et al. (2016) Novobiocin Analogues That Inhibit the MAPK Pathway. *J Med Chem* 59(3):925–933.

131. Blair LJ, et al. (2013) Accelerated neurodegeneration through chaperone-mediated oligomerization of tau. *The Journal of clinical investigation* 123(10):4158–4169.

132. Zhao H, Michaelis ML, Blagg BSJ (2012) Hsp90 modulation for the treatment of Alzheimer's disease. *Adv Pharmacol* 64:1–25.

133. Schulz R, Dobbelstein M, Moll UM (2012) HSP90 inhibitor antagonizing MIF. *Oncoimmunology* 1(8):1425–1426.

134. Jiang F, et al. Optimization and biological evaluation of celastrol derivatives as Hsp90–Cdc37 interaction disruptors with improved druglike properties. *Bioorganic & Medicinal Chemistry*. doi:10.1016/j.bmc.2016.08.070.

135. Zhang T, et al. (2008) A novel Hsp90 inhibitor to disrupt Hsp90/Cdc37 complex against pancreatic cancer cells. *Mol Cancer Ther* 7(1):162–170.

136. Patwardhan CA, et al. (2013) Gedunin inactivates the co-chaperone p23 protein causing cancer cell death by apoptosis. *J Biol Chem* 288(10):7313–7325.

137. Chadli A, et al. (2010) Celastrol inhibits Hsp90 chaperoning of steroid receptors by inducing fibrillization of the Co-chaperone p23. *J Biol Chem* 285(6):4224–4231.

138. Gu M, et al. (2014) Structure-activity relationship (SAR) of withanolides to inhibit Hsp90 for its activity in pancreatic cancer cells. *Invest New Drugs* 32(1):68–74.

139. Yu Y, et al. (2010) Withaferin A targets heat shock protein 90 in pancreatic cancer cells. *Biochem Pharmacol* 79(4):542–551.

140. Sinadinos C, et al. (2013) Low endogenous and chemical induced heat shock protein induction in a 0N3Rtau-expressing Drosophila larval model of Alzheimer's disease. *J Alzheimers Dis* 33(4):1117–1133.

141. Westerheide SD, et al. (2004) Celastrols as inducers of the heat shock response and cytoprotection. *J Biol Chem* 279(53):56053–56060.

142. Yi F, Regan L (2008) A novel class of small molecule inhibitors of Hsp90. *ACS Chem Biol* 3(10):645–654.

143. Ihrig V, Obermann WMJ (2017) Identifying Inhibitors of the Hsp90-Aha1 Protein Complex, a Potential Target to Drug Cystic Fibrosis, by Alpha Technology. *SLAS Discov*:2472555216688312.

144. Mandelkow EM, et al. (1995) Tau domains, phosphorylation, and interactions with microtubules. *Neurobiol Aging* 16(3):355-362-363.

145. Ward SM, Himmelstein DS, Lancia JK, Binder LI (2012) Tau oligomers and tau toxicity in neurodegenerative disease. *Biochem Soc Trans* 40(4):667–671.

146. Iqbal K, Liu F, Gong C-X, Grundke-Iqbal I (2010) Tau in Alzheimer Disease and Related Tauopathies. *Curr Alzheimer Res* 7(8):656–664.

147. Denk F, Wade-Martins R (2009) Knock-out and transgenic mouse models of tauopathies. *Neurobiol Aging* 30(1):1–13.

148. Lewis J, et al. (2000) Neurofibrillary tangles, amyotrophy and progressive motor disturbance in mice expressing mutant (P301L) tau protein. *Nat Genet* 25(4):402–405.

149. Spires TL, et al. (2006) Region-specific Dissociation of Neuronal Loss and Neurofibrillary Pathology in a Mouse Model of Tauopathy. *Am J Pathol* 168(5):1598–1607.

150. SantaCruz K, et al. (2005) Tau Suppression in a Neurodegenerative Mouse Model Improves Memory Function. *Science* 309(5733):476–481.

151. Alamed J, Wilcock DM, Diamond DM, Gordon MN, Morgan D (2006) Two-day radial-arm water maze learning and memory task; robust resolution of amyloid-related memory deficits in transgenic mice. *Nat Protoc* 1(4):1671–1679.

152. Dickey C, et al. (2009) Aging analysis reveals slowed tau turnover and enhanced stress response in a mouse model of tauopathy. *Am J Pathol* 174(1):228–238.

153. Abisambra JF, et al. (2013) Tau accumulation activates the unfolded protein response by impairing endoplasmic reticulum-associated degradation. *J Neurosci* 33(22):9498–9507.

154. Mouton PR, Pakkenberg B, Gundersen HJ, Price DL (1994) Absolute number and size of pigmented locus coeruleus neurons in young and aged individuals. *J Chem Neuroanat* 7(3):185–190.

155. Penley SC, Gaudet CM, Threlkeld SW (2013) Use of an Eight-arm Radial Water Maze to Assess Working and Reference Memory Following Neonatal Brain Injury. *J Vis Exp* (82). doi:10.3791/50940.

156. Giustiniani J, et al. (2014) Immunophilin FKBP52 induces Tau-P301L filamentous assembly in vitro and modulates its activity in a model of tauopathy. *Proc Natl Acad Sci USA* 111(12):4584–4589.

157. Jinwal UK, et al. (2011) The Hsp90 kinase co-chaperone Cdc37 regulates tau stability and phosphorylation dynamics. *J Biol Chem* 286(19):16976–16983.

158. Folch J, et al. (2016) Current Research Therapeutic Strategies for Alzheimer's Disease Treatment. *Neural Plast* 2016:8501693.

159. Bittar A, Sengupta U, Kayed R (2018) Prospects for strain-specific immunotherapy in Alzheimer's disease and tauopathies. *NPJ Vaccines* 3. doi:10.1038/s41541-018-0046-8.

160. Stiegler SC, et al. (2017) A chemical compound inhibiting the Aha1-Hsp90 chaperone complex. *J Biol Chem* 292(41):17073–17083.